Hybrid Nanocontainer with Dual Control Release System

Carolina Matilde Vicente Canadas

Thesis to obtain the Master of Science Degree in

Chemical Engineering

Supervisors: Prof. Dr. José Paulo Sequeira Farinha
Prof. Dr. Carlos Miguel Calisto Baleizão

Examination Committee

Chairperson: Prof. Dr. José Nuno Canongia Lopes
Supervisor: Prof. Dr. Carlos Miguel Calisto Baleizão
Members of the Committee: Profª. Drª. Ana Clara Lopes Marques

November 2021

Declaration

I declare that this document is an original work of my own authorship and it fulfills all the requirements of the Code of Conduct and Good Practices of the Universidade de Lisboa.

Acknowledgments

I would like to express my sincere gratitude to all those who, in some way, allowed this thesis to come true.

First of all, I want to thank my supervisors, Professor Carlos Baleizão and Professor José Paulo Farinha, for the continued support they gave me, for the encouragement, time, patience and, above all, knowledge, that without all this I would not be able to finish this journey.

I would also like to thank José Luís Gonçalves and Tiago Martins, for all the help they gave me in the laboratory, for their shared knowledge, for all their availability and also for their help in characterizing the samples, which would not have been possible without them.

None of this would be possible without the unconditional support of my family, namely my parents and Fábio, during this course and especially during this Master's thesis and, therefore, I would like to thank them very much for all the love, patience and affection they gave me.

I would like to thank all my friends, who were always there during these 5 years and for making my experience better and more memorable. I'm grateful for the sincere friendship and all the memories we have together.

Finally, to FCT-Portugal and COMPETE/FEDER through funding within projects UIDB/00100/2020 and PTDC/CTM-CTM/32444/2017.

Abstract

The aim of this project was to develop novel hybrid mesoporous silica nanoparticles (MSNs) with a double pore system, i.e., containing pores of different sizes and/or structures and functionality. This constitutes a major challenge in the area of smart nanocarriers, allowing the simultaneous loading of different types of cargo, and their release under specified conditions.

To achieve this goal, we tested four different templates in the synthesis of mesoporous silica nanoparticles, using the surfactants hexadecyltrimethylammonium bromide (CTAB), 1-hexadecyl-3-methylimidazolium chloride (Met), 1-hexadecylpyridinium chloride (Pyr) and 1H1H2H2H-perfluorodecylpyridinium chloride (HFDePC). We thus obtained four types of nanoparticles: 1-MSNs-C using CTAB (diameter 69 ± 6 nm), 1-MSNs-Met using Met (diameter 73 ± 10 nm), 1-MSNs-Pyr using Pyr (diameter 64 ± 10 nm) and 1-MSNs-HFDePC using HFDePC (diameter 21 ± 2 nm). To increase the size of the last, several hypotheses were tested, achieving the goal with addition of sodium chloride (NaCl) (diameter 61±10 nm). Removal of the surfactants was evaluated by different methods: calcination, extraction with acidified ethanol (EtOH/HCl), pure tetrahydrofuran (THF), THF with lithium bromide (LiBr) and dichloromethane (DCM), in order to select a pair of templates for the preparation of MSNs with a double pore system with selective removal of each one. None of the extraction processes under study could selectively remove one of the surfactants efficiently. The best methods were 1-MSNs-Pyr extracted with THF and 1-MSNs-HFDePC extracted with EtOH/HCl. CTAB and HFDePC were used to prepare nanoparticles with a double pore system, one without and the other with NaCl, yielding MSNs with diameters of 35±4 and 34±3 nm, respectively. Overall, the novel materials are very promising to develop nanoparticles with a double pore system for selective release.

Key-words: mesopores, silica, nanoparticles, dual pore system, selective release control

Resumo

O objetivo deste projeto foi desenvolver novas nanopartículas híbridas de sílica mesoporosas (MSNs) com um sistema de poros duplos, ou seja, com poros de diferentes tamanhos e/ou estruturas e funcionalidades. Isto constitui um grande desafio, permitindo o carregamento simultâneo de diferentes tipos de carga e a sua liberação em condições específicas.

Para atingir este objetivo, foram testados quatro tensioativos diferentes na síntese de nanopartículas de sílica mesoporosas, utilizando os surfactantes hexadecyltrimethylammonium bromide (CTAB), 1-hexadecyl-3-methylimidazolium chloride (Met), 1-hexadecylpyridinium chloride (Pyr) e 1H1H2H2H-perfluorodecylpyridinium chloride (HFDePC). Assim, obtiveram-se quatro tipos de nanopartículas: 1-MSNs-C utilizando CTAB (diâmetro 69 ± 6 nm), 1-MSNs-Met utilizando Met (diâmetro 73 ± 10 nm), 1-MSNs-Pyr utilizando Pyr (diâmetro 64 ± 10 nm) e 1-MSNs-HFDePC utilizando HFDePC (diâmetro 21 ± 2 nm). Para aumentar o tamanho da última, foram testadas várias hipóteses, atingindo o objetivo com adição de cloreto de sódio (NaCl) (diâmetro 61 ± 10 nm). A remoção dos tensioativos foi avaliada por diferentes métodos: calcinação, extração com etanol acidificado (EtOH/HCl), tetrahidrofurano puro (THF), THF com brometo de lítio (LiBr) e diclorometano (DCM), com a finalidade de selecionar um par de tensioativos para a preparação de MSNs com sistema de poro duplo com remoção seletiva de cada um. Nenhum dos processos de extração em estudo conseguiu remover seletivamente um dos tensioativos de forma eficiente. Os melhores métodos foram 1-MSNs-Pyr extraído com THF e 1-MSNs-HFDePC extraído com EtOH/HCl. CTAB e HFDePC foram utilizados para preparar nanopartículas com um sistema de poro duplo, uma sem e outra com NaCl, resultando em MSNs com diâmetros de 35 ± 4 e 34 ± 3 nm, respetivamente. No geral, os novos materiais são muito promissores para o desenvolvimento de nanopartículas com sistema de poro duplo para liberação seletiva.

Palavras-chave: mesoporos, sílica, nanopartículas, sistema duplo de poros, controlo de libertação seletiva

General Contents

Figures Index

Tables Index

Abbreviations List

1-MSNs	Mesoporous Silica Nanoparticles with One Template
2-MSNs	Mesoporous Silica Nanoparticles with Two Templates
BET	Brunauer-Emmett-Teller method
BJH	Barrett-Joyer- Halenda method
CMC	Critical Micellar Concentration
CPP	Critical Packing Parameter
CTAB	Hexadecyltrimethylammonium Bromide
DCM	Dichloromethane
D_{TEM}	Diameter obtained by Transmission Electronic Microscopy
EtOH	Ethanol
EtOH/HCl	Acidified Ethanol
FIL	Fluorinated Ionic Liquid
H_2O_2	Hydrogen Peroxyde
HCl	Hydrochloric Acid
HFDePC	1H1H2H2H-perfluorodecylpyridinium chloride
IL	Ionic Liquid
LiBr	Lithium Bromide
MCM-41	Mobil Composition of Matter Number 41
MCM-48	Mobil Composition of Matter Number 48
MCM-50	Mobil Composition of Matter Number 50
Met	1-Hexadecyl-3-methylimidazolium Chloride
MSN	Mesoporous Silica Nanoparticle
NaCl	Sodium Chloride
NaOH	Sodium Hydroxide
NP	Nanoparticle
Pyr	1-Hexadecylpyridinium Chloride
TEM	Transmission electron microscopy
TEOS	Tetraethoxysilane
THF	Tetrahydrofuran

Unit List

°C	Degree Celsius
g; mg	Grams; milligrams (10^{-3} g)
h; min; s	hours; minutes; seconds
L; mL	Litre; millilitre (10^{-3} L)
M; mM	Molar; millimolar (10^{-3} M)
m, cm, µm, nm	meter; centimeter (10^{-2} m); micrometer (10^{-6} m); nanometer (10^{-9} m)
rpm	Rotations per minute
x g	Times gravity

1. Introduction

Nanotechnology is the manipulation and understanding of matter and processes at the nanoscale, below 100 nm in one or more dimensions. At this size, materials begin to exhibit unique properties that affect physical, chemical, and biological behavior which leads to many novel applications, such as in medicine, chemistry, electronics, energy, etc. [1]

The rapidly developing fields of nanotechnology and general processes for generating, manipulating, and utilizing nanomaterials have attracted considerable attention in recent years and opened up a promising era in the fields of bioanalysis, biotechnology, and biomedical applications. [2,3]

1.1. Nanoparticles

Nanoparticles (NPs) have unique physical (structure, electronic, magnetic and optical, compatibility), chemical (catalytic) and electrochemical properties, a series of research activities focus on the synthesis and functionalization. From different kinds of metal NPs to semiconductor NPs, numerous types of NPs have arisen to meet a wide scope of specific applications. In particular, the utilization of functionalized NPs as carriers or labels, markers and probes have shown great success in bioimaging, biomarkers and biosensing, and diagnostic and therapeutic purposes because of their adjustable and customizable properties.[3] For example, functionalized gold nanoparticles have been used to develop DNA and protein biosensors that combine colorimetric, scanning, and electrochemical techniques.[2,3] Quantum dots have been used to develop various optical, electrochemical, electrochemiluminescence, chemiluminescence biological assays.[2] These nanoparticles through controlled composition and surface modification enhance the detection signal, improve sensitivity, reduce detection time, produce better repeatability, and bring a series of new applications.[2,3]

Nanoparticles are materials with at least one dimension and size between 1-100 nm. According to their composition (Figure 1, adapted from references 4,5) they can be classified as organic (such as polymeric nanoparticles, liposomes, etc.), inorganic (such as silica, gold, magnetic nanoparticles, etc.) and hybrid (composed of two or more materials, such as silica nanoparticles with a polymeric shell). [1,4,6–8]

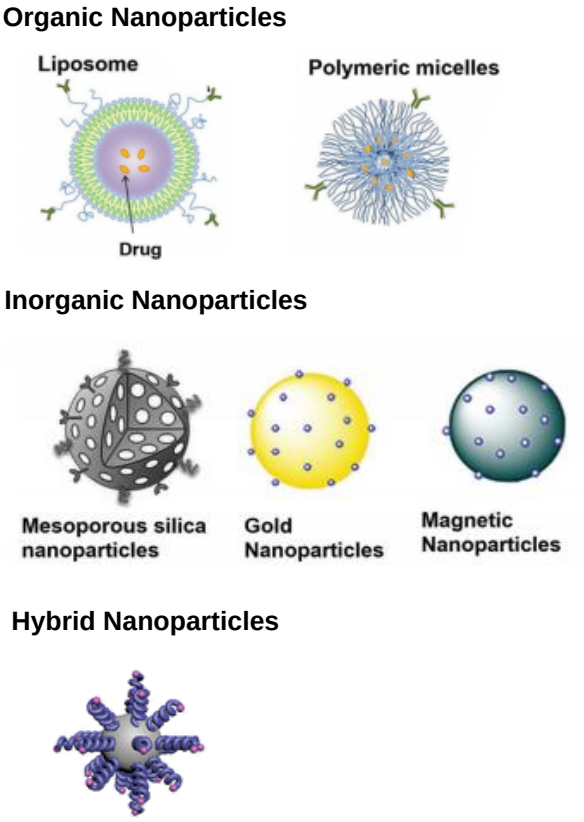

Figure 1: Nanoparticles' classification according to their composition. Adapted from 4 and 5.

Nanoparticles' size affects their physical and chemical properties such as surface area and mobility (the smaller the greater the mobility, for example). At smaller sizes the quantum effects are extremely important and the optical properties are dominant. [1,6,7]

Although they are very promising for many types of applications, there are still concerns in the use of these materials related to health or the environment. These should be considered in such a way that the use NPs become more environmentally friendly and more convenient. [1,9]

1.2. Silica Nanoparticles

Silica nanoparticles have properties that make them increasingly important in several areas. These NPs are robust, biocompatible, non-toxic, thermally and chemically stable, electronegative in aqueous media at neutral pH, mechanically stable, protect and stabilize embedded molecules, are easy to prepare, exhibit good monodispersity, have high specific surface area and, finally, their surface can be functionalized due to an high surface silanol concentration.[3,10,11]

Spherical silica nanoparticles can have diameters ranging from a few tens of nanometers to micrometers. By changing the reaction conditions, such as the concentration of reactants, the pH, and the reaction temperature, the sizes of the particles can be easily tuned.[10]

The main applications of silica nanoparticles are in:

I. Catalysis, in which they provide ideal sites for executing highly specific chemical transformations, offering increased efficiency and enhanced selectivity over other catalytic systems;[12]
II. Corrosion, in which they are used in coatings for the passivation of surfaces against corrosion; [12]
III. Drug and gene delivery and biomedicine, such as protein adsorption and separation, nucleic acid detection and purification, theragnostic platform and imaging contrast agents construction. [2,3,10,13,14]

On the other hand, the size and high surface area of these particles, despite being advantageous for many applications, can lead to their aggregation, making it difficult to handle in liquid and dry forms. It is necessary to overcome these difficulties so that this type of materials can be commercialized and, consequently, used clinically, in corrosion and catalysis applications. [6] One way to improve this is to make the external functionalization of the nanoparticle so that the colloidal stability increases, as the repulsion between particles will increase.[15]

Silica nanoparticles can be obtained in compact form or with a mesoporous network. For the synthesis of compact NPs, the Sol-Gel method[16] or the Stöber method[17] can be used. For mesoporous nanoparticles the so-called modified Stöber method is used.[18]

1.2.1. Synthesis by the Sol-Gel Method

This method is used to produce silica, glass and ceramic materials in general, since mild conditions are used and the materials obtained exhibit low dispersity.[16] In this process, the development of networks occurs through the arrangement of a colloidal suspension, which is called sol, and the formation of gel that forms a system in continuous liquid phase. That said, a sol is a stable colloidal dispersion of particles, usually 1-100 nm, in a liquid, whereas a gel is an interconnected solid porous network. Several types of precursors can be used, divided into two categories: inorganic, which includes sodium silicate (Na_2SiO_3), etc., and alkoxides, which include TEOS (tetraethyl orthosilicate), TMOS (tetramethoxysilane) , etc. [16,19]

The sol process involves two main steps: hydrolysis and condensation. It starts with a precursor of silica, in the presence of an acid catalyst, for example hydrochloric acid (HCl), or basic, for example, ammonium hydroxide (NH_4OH) or sodium hydroxide (NaOH), where a one-phase solution is formed which undergoes a solution-to-gel transition to form a two-phase rigid system that contains solid metal oxides and solvent-filled pores. The materials obtained depend on the nature of the catalyst used. For example, if a silica alkoxide is used as a precursor, when an acid catalyst is added, linear polymers are weakly bounded together, which mix and form more branches and lead to the formation of a gel. If a basic catalyst is used, since the reactions kinetics' are faster, highly branched clusters are formed. These differences are due to the fact that their solubility in the medium depends on the pH, that is, in basic medium they are more soluble which favors more interconnection between clusters than in acidic medium. The condensation step occurs between two groups -OH or Si-OH and an alkoxy group or between to alkoxy groups to form a Si-O-Si network and a water or alcohol molecule, respectively. [16,19,20] General equations of hydrolysis and condensation steps (*1*), (*2*) e (*3*) are shown below: [16,19,20]

$$Hydrolysis: Si-\ OR_4 + H_2O \rightleftarrows Si-(OR)_3(OH) + ROH \quad (1)$$

$$Water\ condensation: (OR)_3-Si-OH\ +\ HO-Si-(OR)_3 \rightarrow [(OR)_3Si-O-Si(OR)_3] + H_2O \quad (2)$$

$$Alcohol\ condensation: (OR)_3-Si-OR\ +\ HO-Si-(OR)_3 \rightarrow [(OR)_3Si-O-Si(OR)_3]\ +\ R-O-H \quad (3)$$

These reactions are initiated in several active centers and from the moment that in one of these centers there is a significant number of Si-O-Si bonds, they interact and form colloidal particles.[19] Then, depending on the conditions, particles of silica or a network of silica gel are formed, as shown in Figure 2. [16]

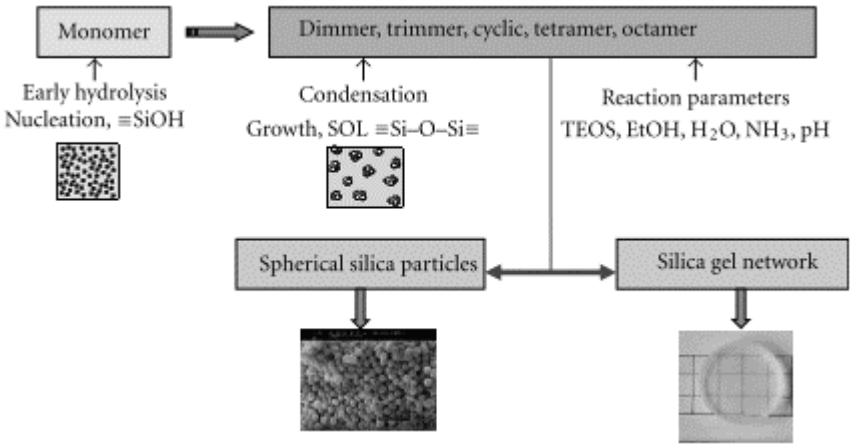

Figure 2: Schematic diagram of silica formation by the sol-gel process. Adapted from 16.

1.2.2. The Stöber Method

As mentioned in section 1.2.1, when the sol-gel synthesis takes place in a basic medium, individual particles are formed, which facilitates the formation of spherical silica particles. In 1968, Stöber *et all.* Described a method to obtain spherical and compact silica particles, using silica alkoxides as precursors, ammonia as catalyst and water, in low molecular weight alcohols as solvent. Particles with sizes between 5-2000 nm were obtained, depending on the conditions used, exemplified in Figure 3. [17,18,21,22]

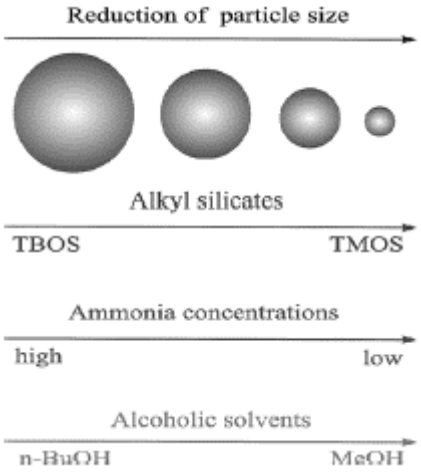

Figure 3: Influence of the type of the tetraalkyl orthosilicate, the ammonia concentration, and the alcoholic solvent on the size of the silica particles produced by the Stöber method. Silica nanoparticles decrease in size when, in the synthesis, are used tetraalkyl orthosilicates used with smaller chains, lower ammonia concentrations and smaller alcohol chains. Adapted from 18.

The size and morphology of these particles can be controlled by the hydrolysis and condensation kinetics, and by the growth and aggregation of the particles.[22] The major factor controlling these variants is the pH of the medium, since it has influence on the charges of silica species, which in turn influence the rates of hydrolysis and condensation (Figure 4).

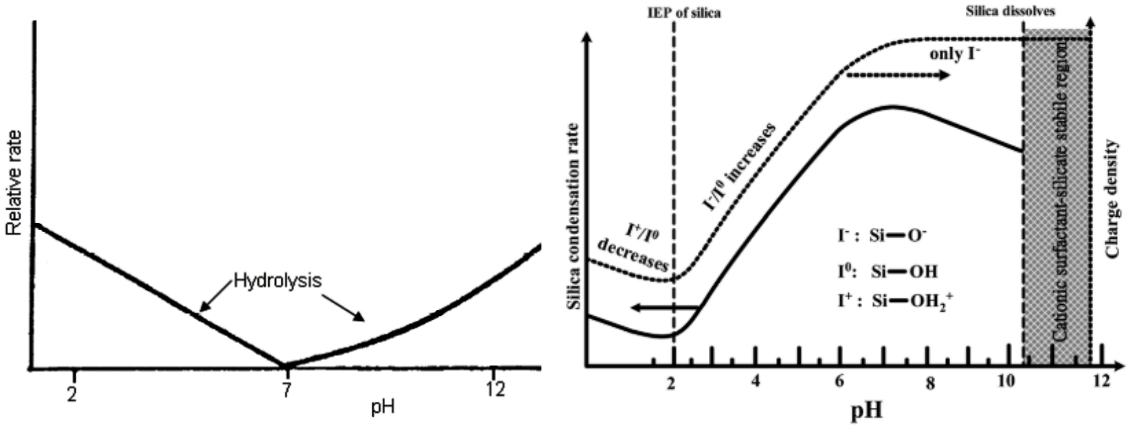

Figure 4: Variation on hydrolysis rate (left) and condensation rate and charge density (right) with pH. Adapted from references 25 and 23, respectively.

The hydrolysis could be catalyzed by acid or base, with the properties of the resulting materials depending on the catalyst used. This step creates multiple particle nuclei that will grow when condensation starts to occur, producing uniform nanoparticles. The silica species are positively charged in pHs below the isoelectric point, in this case pHs 2.0, so that the charge density increases as the pH decreases (Figure 4, right). When the pH value is higher than the isoelectric point, the silica species became negative (silicates), and the charge density increases with the pH. High pH values favor the nucleophilic attack of the negatively charged silicates, which will increase the condensation kinetic. Around a pH 7.5 the condensation rate reaches a maximum value. Above that value the silicates will be gradually more instable, and so, the condensation rate decreases.[22–25]

1.2.3. Synthesis of Mesoporous Silica Nanoparticles

Mesoporous silica nanoparticles (MSNs) have aroused great interest in the scientific world, due to their unique properties. MSNs have ordered pore structure in the short and long range, high surface area and pore volume (which depends on the template used) and controllable particle size. The particle surface and the external pore walls can be selectively functionalized to prevent aggregation or to load molecules for drug delivery, for example. Also, they have good biocompatibility, which means that they are safe for humans, animals and nature.[26] These particles are also easy to synthesize and are very thermally and chemically stable. [27]

The synthesis of the first silica mesoporous arrays with an ordered structure and a uniform pore size was made in 1992 by scientists from Mobil Corporation.[28] This family of materials has been given

the name M41S. These materials have pore diameters between 2 and 10 nm and amorphous walls. Within this class there are several types of nanoparticles, the best known are MCM-41 which have a hexagonal pore structure, MCM-48, which have a cubic arrangement and MCM-50, with lamellar structure, as shown in Figure 5. [26,28,29]

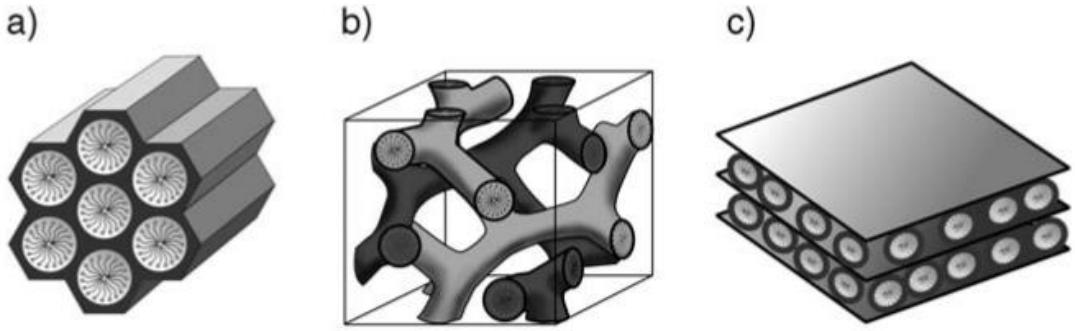

Figure 5: Structures of the M41S family where a) is MCM-41, b) is MCM-48 and c) is MCM-50. Adapted from 29.

This materials can have pores between 2-10 nm, pore volume above 1mL/g and particle size between 10 and 100 nm.[30]

The synthesis of mesoporous silica nanoparticles (MSNs) is classified as a modified Stöber method, that is, the difference to the original method is the use of a template, usually surfactants, to form pore structures and there is also a change in some compositions in the synthesis. These surfactants have a hydrophilic part and a hydrophobic part and, therefore, when they are in water, they tend to form micelles so that the hydrophobic part is protected and only the hydrophilic part contacts the water, this phenomenon is due to hydrophobic effects. These structures are formed when the surfactant concentration is above the CMC (critical micellar concentration. [13,18–20,31]

The surfactant can form several 3D structures depending on its geometry, which can be predicted according to its CPP (critical packing parameter):

$$CPP = \frac{v}{a_0 l_c} \quad (4)$$

Where v is the volume of the hydrophobic part, a_0 is the effective area of the hydrophilic part and, finally, l_c is the length of the hydrophobic part.

According to the CPP value for each type of surfactant, it is possible to know which aggregate forms they'll take, for example, spherical micelles are obtained when CPP <1/3, cylindrical micelles when 1/2 <CPP> 1/3, among others.[32] For the formation of MSNs of the type MCM-41 it is necessary to form cylindrical micelles, with CTAB (cetyltrimethylammonium bromide), being one of the most used cationic surfactants.

The synthesis of these particles begins with the formation of cylindrical micelles that aggregate in a hexagonal form depending on the stability of the medium. The less stable, the greater the aggregation and, consequently, the final size of the particles. This stability is modified by the addition of the basic catalyst in different concentrations, since it neutralizes the surface charges of the micelle polar part. After the formation of these structures, the precursor of silica is added, which has a greater affinity with the surface of the micelles than with itself due to the fact that in basic pH silica deprotons after hydrolysis, taking a negative form what causes it to bind to the positive charges of micelles and, therefore, the reactions of hydrolysis and condensation occur in these active centers, thus forming the MSNs. It should be noted that depending on certain conditions of synthesis these nanoparticles will be larger or smaller, for example, the amount of silica precursor, pH, reaction time, temperature, etc. It was concluded that pH is the parameter that most influences the size of MSNs, as previously mentioned. With high pH values, after the hydrolysis of the silica precursor, there are more OH^- groups to interact with the positive charges on the surface of the micelle, decreasing its stability in the medium, which in turn induces the aggregation of the formed micelles and, consequently , forms larger nanoparticles and vice versa.[13,26,33] This process is illustrated in Figure 6.

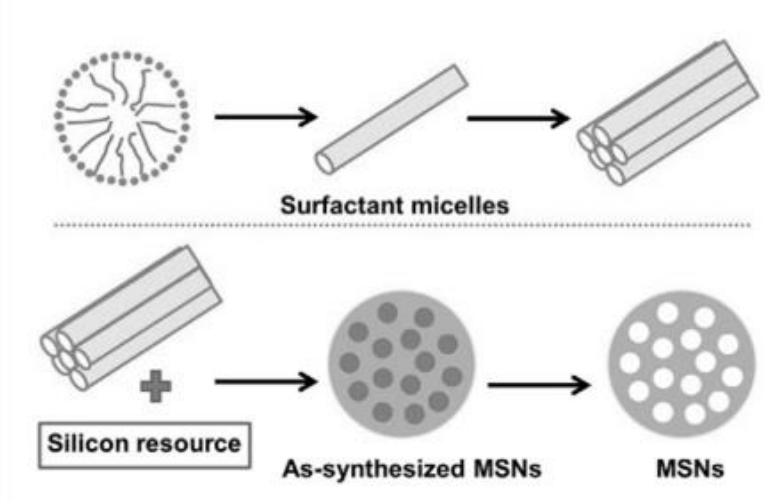

Figure 6: Illustration of the synthesis of mesoporous silica nanoparticles. Adapted from 26*.*

At pH values between 2 and 7 the silicates will tendentially assemble with the positively-charged surfactants or neutral polymers, by electrostatic and hydrogen bonding interactions. At pH values above 7, silicates with a high negatively-charged density will assemble with the cationic surfactants through strong electrostatic interactions. The most of MSNs synthesis occur at pH above 10.5 since it is a value that combines a favored hydrolysis and a fast condensation. [22–25]

1.3. Template Removal

To make the pore network of the MSNs available it is necessary to remove the template to accommodate molecules or polymers. [34–36]

After removing the template, the MSN structure should be stable, with unblocked pores, which is analyzed by nitrogen adsorption. It is also important to achieve a low cost, low time consuming and environmentally friendly template removal.[34–36] The best-known processes for removing the template are calcination and solvent extraction.

1.3.1. Calcination

Calcination is the most used method for removing templates from MSNs. It is typically completed under an air atmosphere at approximately 500°C. It is a simple and effective method, since it completely removes the template and also consolidates the silicate framework by thermal condensation. Despite these advantages, there are still some problems: agglomeration of colloidal particles and structural shrinkage; partial destruction of the ordered structure can occur; and, finally, as the silanol groups condense at high temperatures there is a significant reduction of silanols on the surface. In the case of nanoparticles with organic functionalities, this method cannot be used since they would be removed together with the template.[34–37]

There are less conventional calcination methods such as rapid calcination or microwave-assisted calcination. In rapid calcination, as the name implies, samples undergo intensive calcination with high-rate heating.[34] In microwave-assisted calcination, templates can be eliminated in just a few minutes, but in return special high-temperature-proof reaction vessels are needed.[36] These two methods are not yet widely implemented as they need extra care and are more expensive.[34,36]

1.3.2. Solvent Extraction

One of the alternative methods to calcination is solvent extraction, usually performed with an organic solvent at low pH such as ethanol acidified with hydrochloric acid. Organic solvents at low pH values cause the silica to protonate, which leads it to its neutral state, decreasing the silica-template interactions.[38,39] This method has some advantages over the previous method, since it can maintain a large amount of silanol groups and also maintain the initial pore structure without significant shrinkage. The extraction can be applied to materials with organic functionalities since it allows the removal of the template without decomposing the organic part. [34–36]

Despite the various advantages, this method is time consuming, it requires an organic solvent which at an industrial level can represent a very high cost since large quantities of solvent are required, raising environmental concerns. For biomedical applications it is necessary that the total removal of solvent and template is ensured, due to possible toxicity.[34–36]

1.3.3. Other Methods

There are some lesser used template extraction methods, such as hydrogen peroxide treatment, supercritical fluid extraction, etc.[36]

H_2O_2 treatment is based on oxidation processes, in which there is total degradation of organic compounds resulting from the generation of hydroxyl radicals ($HO^{\bullet}$) in situ. This type of radical is very strong and is a non-selective oxidizer which makes it capable of degrading a vast number of organic compounds and transforming them into carbon dioxide and water. [34,36,40] All treatments based on hydroxyl radicals have advantages:[34]

I. The silica framework does not shrink or it shrinks in a very small way, which leads to larger surface areas and larger pore volumes;

II. After treatment, the surface continues with a large amount of silanol groups.

When a metal ion is added to the samples to generate HO • radicals, a Fenton reaction occurs, for example:[34]

$$Me^{2+} + H_2O_2 \rightarrow Me^{3+} + HO^{\bullet} + OH^{-} \quad (5)$$

$$Me^{3+} + H_2O_2 \rightarrow Me^{2+} + HO_2^{\bullet} + H^{+} \quad (6)$$

Despite the previously announced advantages, the Fenton reaction has some disadvantages, such as, the reaction time is long since it can reach 24 hours or more and also the fact that at the end of the reaction there is the presence of residual metal from the ion used in the silica framework, which can then limit some applications of these nanoparticles.[34]

When only hydrogen peroxide is used, it must have sufficient oxidizing power to be able to remove the template. To achieve this, the temperature is raised and the reaction is carried out at very high temperatures in a reflux state. This technique only has the disadvantage of being very time consuming. [34,40]

Supercritical fluids have low viscosity, high diffusivity and density. Thus, the diffusion coefficients of solutes in these fluids are higher than those in normal liquids and mass transfer is more efficient. The most used supercritical fluid is CO_2 since it has critical properties (TC=31.1°C, PC=72 bar) that are suitable for most extraction applications, have low toxicity and it is low cost.[41] This method have

some advantages, such as the final mesoporous material possess more uniform pore size and larger pore diameter. Moreover, this type of extraction is done in a shorter time with lower volumes of solvent required. [41] The main disadvantage of this method is the expensive equipment and process analysis.

1.3.4. Nitrogen Adsorption Analysis

To analyze the final nanoparticles, it is necessary to do a nitrogen adsorption analysis, by the BET (Brunauer-Emmett-Teller) and BJH (Barrett-Joyer- Halenda) method, in which the surface area is obtained in the first, and the pore volume and pore diameter in the second. Both in BET and in BJH methods, nitrogen is usually used because of its high purity and strong interaction with most solids. Since the interaction between the gas phase and the solid phase is generally weak, liquid nitrogen is used to cool the surface to obtain a detectable amount of adsorption. The BJH method calculates the pore size distributions from experimental isotherms using the Kelvin model of pore filling, i.e., the gas pressure is increased incrementally until all pores are filled with liquid. Next, the gas pressure is reduced incrementally, evaporating the condensed gas from the system. [42–44] In BET a known amount of nitrogen is gradually released into the sample cell. Relative pressures below atmospheric pressure are achieved by creating partial vacuum conditions. After the saturation pressure, no matter whether the pressure is further increased, no more adsorption occurs. After the adsorption layer is formed, the sample is taken out of the nitrogen atmosphere and heated, so that the adsorbed nitrogen is released from the material and quantified (desorption). The quantity of gas adsorbed is plotted as a function of the relative pressure. There are five types of adsorption isotherms: [44–46]

I. Type I - Typical of microporous materials, where the pores slightly exceed the molecular diameter of the adsorbate.
II. Type II – The most common to be found in adsorption measurements and occur in non-porous systems.
III. BET method does not apply because no monolayer is formed.
IV. Typical of samples with pores in the range of mesopores to macropores, in which the formation of adsorption multilayers is possible, but the size of the porosity of the material is limited.
V. Similar to type IV isotherms but it is not possible to identify the occurrence of formation of the first adsorption layer and therefore are not applicable to BET.

The isotherms illustrations are shown in Figure 7.

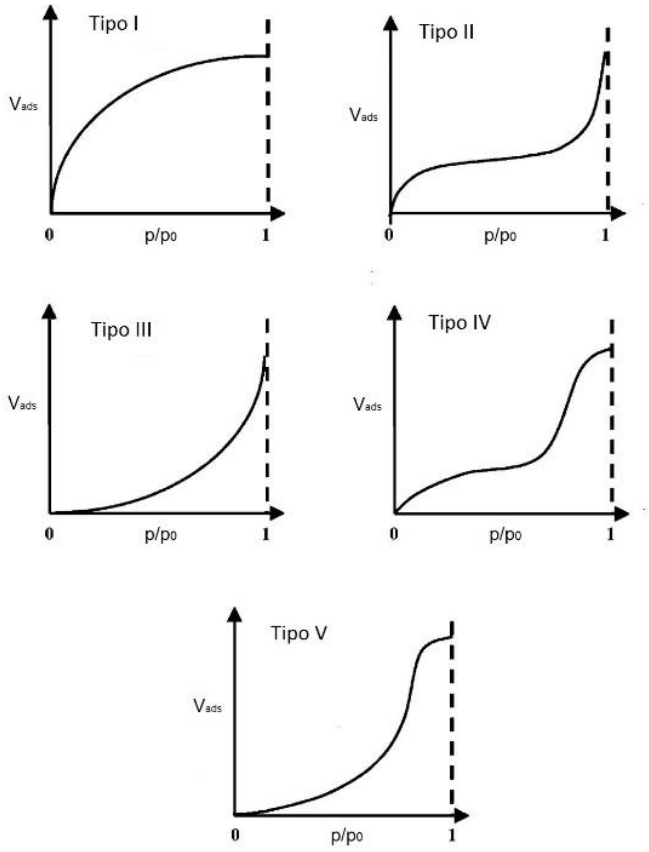

Figure 7: Isotherm types for physical adsorption: Plots the volume of gas adsorbed onto the surface in function of the relative pressure Adapted from 46.

1.4. Mesoporous Silica Nanoparticles with a Double Pore System

Mesoporous silica nanoparticles with a double pore system are very interesting materials. Unlike nanoparticles with only one type of pore they can have pores of different sizes or structures, load several types of molecules, from drugs to proteins and nucleic acids, for example. These materials offer the possibility to functionalize the nanoparticle surface, as well as the surface of each type of pore selectively.[47,48]

This type of material can be synthesized in two ways: one-step synthesis or two-step synthesis. The first strategy is very similar to the synthesis of MSNs with only one pore type (described in chapter 1.2.3) the only difference is that instead of one template, two are used and these two must form independent cylindrical micelles. An example of the one-step synthesis, where CTAB was mixed with an amphiphilic block copolymer (PS-b-PAA), is shown in Figure 8.

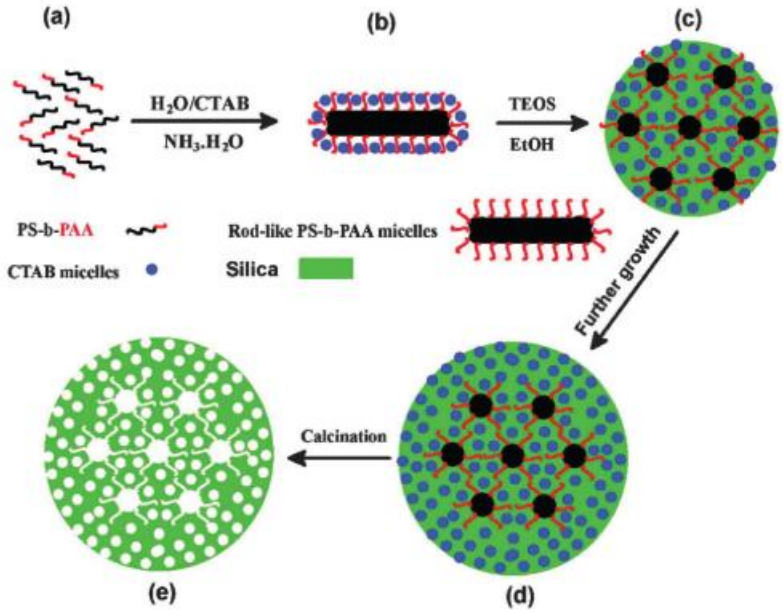

Figure 8: Schematic representation of the one-step synthesis where: (a) THF solution of PS-b-PAA; (b) CTAB-coated PS-b-PAA aggregates; (c) Core part formed from the assembly between CTAB-coated PS-b-PAA aggregates and TEOS; (d) Mesoporous shell formation via the self-assembly between the remaining CTAB and the additional TEOS; (e) Final core-shell structured dual-mesoporous silica spheres after removing the templates. Adapted from 51*.*

The second strategy involves the formation of a primary mesoporous silica network (primary particle), exactly like the synthesis of MSNs with one pore which are added to a solution with the second template, as shown in Figure 9. [47–53] The primary particles involve the micelles of the second template, a structure is formed that grows and forms two types of pores. The connection between the two steps is achieved by hydrogen bonds between the silanol groups of silica and the hydrophilic heads of the chains of the second template.[47–53]

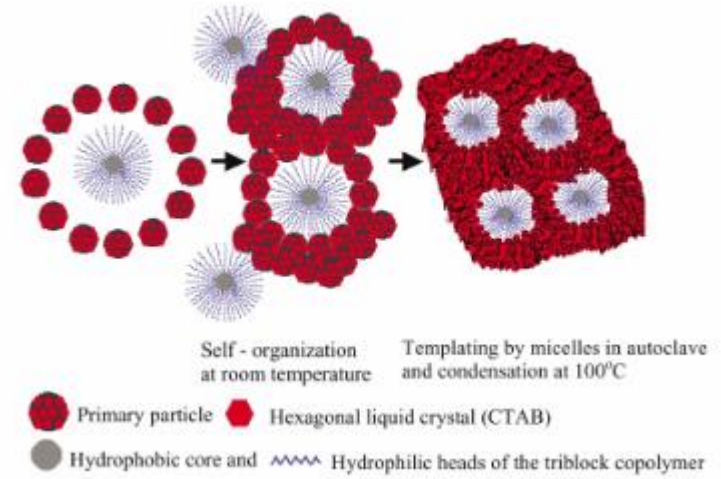

Figure 9: Schematic representation of the second step of the two-step synthesis. Copied from 53.

When using the one-step synthesis, it must be taken into account that the two templates used must have sufficiently different properties so that mixed micelles do not form.[54] When using two-step synthesis, the pore size can be controlled independently, since they are formed in different steps, but the second template must have an affinity for the silica network formed in the first step so that it is able to bind and form the core-shell type particle.[52]

Although the previous methods are really promising, the two templates are removed at the same time, which makes it only possible to load pores with the same molecule or functionalize both types of pores in the same way. This limits the advantages of these materials. To overcome these disadvantages, it is necessary to selectively remove the two templates, which will open doors to a wide range of applications, at a lower cost.

1.5. Objectives and Work Strategy

The aim of this project is to develop a hybrid nanocontainer based on mesoporous silica nanoparticles with a double pore system for selective release control. These materials have been gaining great interest in the scientific community, since they have advantages over nanoparticles with only one type of pore or even over nanoparticles with a double pore system with the templates extracted at the same time. These NPs have pores of different sizes or structures, and so it is possible to load different types of molecules (from drugs to proteins and nucleic acids, etc.), and it is also possible to functionalize the surface of these materials as well as the surface of each type of pore selectively. [47,48] For these reasons the potential of these materials is very high, with applications in catalysis, delivery, corrosion and energy. The main interest is that the two templates can be extracted selectively so that it is possible to take full advantage of this double pore system (Figure 10).

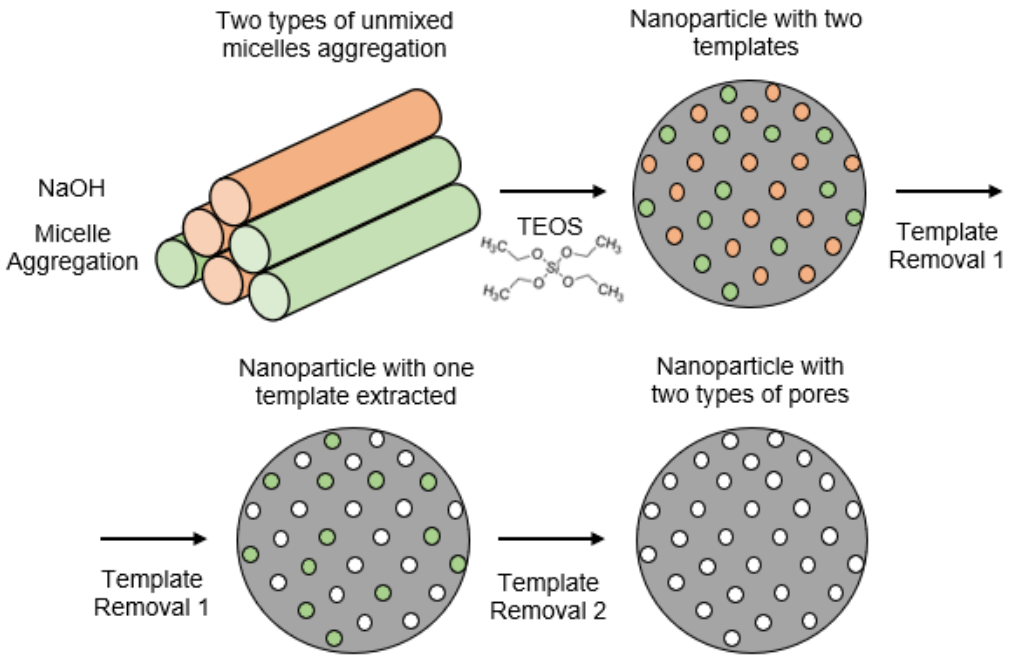

Figure 10: Schematic illustration of a hybrid nanocontainer based on mesoporous silica nanoparticles with a double pore system for selective release control.

To find the ideal pair of templates that would be selectively removed it is necessary to test several templates and to study different extraction methods.

Firstly, MSNs with only one template will be prepared, using four surfactants with different characteristics, in order to be selectively removed: hexadecyltrimethylammonium bromide (CTAB), a cationic surfactant, 1-hexadecyl-3-methylimidazolium chloride (Met) and 1-hexadecylpyridinium chloride (Pyr), both ionic liquids (IL), and finally, a fluorinated surfactant, 1H1H2H2H-perfluorodecylpyridinium chloride (HFDePC).

Ionic liquids are molten salts at room temperature, which have unique characteristics such as low vapor pressure, wide liquid temperature range, mild reaction condition, solvation ability, easy recycle ability and thermal stability.[50,55,56] These compounds are formed by an ionic part and an alkyl part, which gives them great amphiphilicity, and can form extended hydrogen bonds between molecules in the liquid state, which is the basis of self-assembly processes and, therefore, they can easily aggregate and produce micelles in an organized way.[47,49,50] For the reasons mentioned above, ionic liquids used as templates have generated great interest among the scientific community.

Fluorinated surfactants behave similarly to their hydrocarbon analogues and therefore form micelles, vesicles or lamellar phases depending on their geometry and chemical structure.[55] For the purpose of this work, it is important that these surfactants form cylindrical micelles. These compounds are more hydrophobic than their hydrocarbon analogues which results in lower surface tension and therefore lower CMC. The presence of fluor results in bulkier and stiffer chains with high electron density,

which pack more easily because the chains are all in their trans state. Based on the CPP of these compounds, equation (*4*), it is known that they tend to form aggregates with lower curvature than hydrocarbon surfactants, since their chains have a greater volume. [55,57–59]

The structure of each surfactant is shown in Figure 11, Figure 12, Figure 13 and Figure 14.

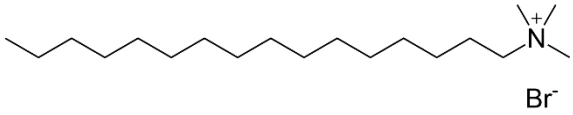

Figure 11: Hexadecyltrimethylammonium bromide (CTAB) molecular structure. Copied from reference 59.

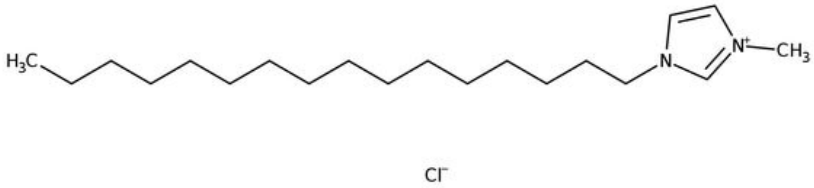

Figure 12: 1-hexadecyl-3-methylimidazolium chloride (Met) molecular structure. Copied from reference 56.

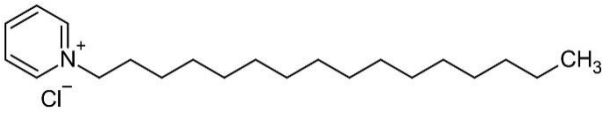

Figure 13: 1-hexadecylpyridinium chloride (Pyr) molecular structure. Copied from reference 59.

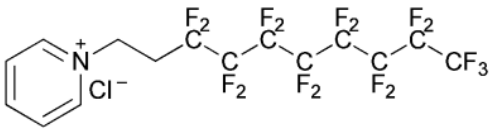

Figure 14: 1H1H2H2H-perfluorodecylpyridinium chloride (HFDePC) molecular structure. Copied from reference 56.

The fact that the surfactants are different is important because in the synthesis with two templates (2-MSNs) they will have higher probability of not forming mixed micelles. Also, increasing the probability of being selectively extracted.

In order to achieve a selective template extraction, it is necessary to test different extraction methods to see which could extracts one of the templates, but not the others. Calcinations have to be performed as a basis of comparison. Various solvent extractions will also be performed using solvents from different families, i.e., ethers, alkanes, chlorinated chains, alcohols, etc. The most suitable solvents for this study are tetrahydrofuran (THF), hexane, dichloromethane (DCM) and acidified ethanol (EtOH/HCl).

Finally, in order to make nanoparticles with a double pore system it is necessary to choose the pair of surfactants that will not form mixed micelles and that can be selectively.

2. Experimental Part

2.1. Materials

The following materials were used without further purificaton: 1-hexadecyl-3-methylimidazolium chloride (98%, IOLITEC), 1-hexadecylpyridinium chloride (98%, IOLITEC) hexadecyltrimethylammonium bromide (99 % CTAB, Sigma), 1H, 1H, 2H, 2H-heptadecafluorodecyl Iodide (98%, TCI), pyridine (99% Pyridine, Sigma-Aldrich), diethyl ether (99.8%, ACS reagent, Honeywell), acetone (99% Acetone for spectroscopy, Acros Organics), methanol (ACS reagent, Sigma-Aldrich), Amberlite IRA-410 chloride form (Sigma-Aldrich), sodium hydroxide (Pure NaOH, PanReac AppliChem), sodium chloride (NaCl, PanReac AppliChem), tetraethoxysilane (98 % TEOS, Aldrich), hydrochloric acid (37 % HCl, HCl fuming, 37% ACS reagent, Sigma-Aldrich), absolute ethanol (99.9 % EtOH, Scharlau), lithium bromide (LiBr, Sigma-Aldrich), tetrahydrofuran (ACS reagent, THF, Carlo Erba Reagents) and dichloromethane (99.95% DCM, José Manuel Gomes dos Santos, Lda). The deionized (DI) water was generated using a Millipore Milli-Q system (≥18 MΩcm, Merck, NJ, USA).

2.2. Equipment

2.2.1. Centrifuge

To clean the MSNs was used an Avanti J – 30I Centrifuge (Beckman Coulter, California, USA), rotor JA – 30.50 Ti, in which were used 50 mL centrifuge tubes from the same manufacturer. For washing MSNs after template removal was used a Centrifugal Refrigerator (3-16K) (Sigma Zentrifugen, Osterode am Harz Germany), rotor 12141, in which 10 mL polypropylene tubes were used for the centrifugations.

2.2.2. Transmission Electronic Microscopy (TEM)

TEM images were obtained on a Hitachi transmission electron microscope (Hitachi High – technologies, Tokyo, Japan), model H-8100, with a LaB_6 filament (Hitachi) complemented with an accelerator voltage of 200 kV. A camera KeenView (Soft Imaging System, Münster, Germany) is a part of this equipment, which through iTEM software, allows acquiring TEM images. To analyze MSNs, the particles are dispersed in ethanol and then prepared and dried on a carbon grid. The size/dimension, polydispersity, and morphology of the particles were obtained by measuring at least 50 nanoparticles by Image J software.

2.2.3. Nitrogen Adsorption

To characterize the MSNs and their pores it was performed nitrogen adsorption (BET). The N_2 adsorption–desorption isotherms were obtained at 77 K of the degassed samples, using a Micromeritics ASAP 2010.

2.3. Methods

2.3.1. Fluorinated Surfactant (HFDePC) Synthesis

The fluorinated surfactant, 1H1H2H2H-perfluorodecylpyridinium chloride (HFDePC), was synthesized according to the literature[60]. 5 g of 1H1H2H2H-heptadecafluorodecyl Iodide were dissolved in a pyridine solution and then the mixture was refluxed for 30 minutes. Afterwards, with the heating and stirring turned off, the mixture cooled down and formed yellow precipitates. These precipitates were filtered with diethyl ether, recrystallized from acetone and filtered again with acetone. The filtered solids were left to dry in the oven for 24 hours so that the greatest amount of solvent would evaporate. Then, it was made an ionic exchange for 24 hours twice, joining resin (Amberlite IRA-410 chloride form) with the precipitated solid and with enough methanol so that constant agitation is possible. Finally, on a rotary evaporator as much methanol as possible was evaporated from the solution of the previous step and then it was left to dry in vacuum for 24h.

2.3.2. Single Template MSNs (1-MSNs)

2.3.2.1. Mesoporous silica nanoparticles synthesis

1-MSNs were synthetized by the modified Stöber method reported in the literature[30]. In a 500 mL polypropylene flask, 240 mL of deionized (DI) water and surfactant were added. Depending on the final particles desired were used 500 mg of CTAB (1-MSN-C), 771 mg of HFDePC (1-MSN- HFDePC), 998 mg of HFDePC (1-MSN- HFDePC (7.2 mM)), 471 mg of Met (1-MSN-Met) or 466 mg of Pyr (1-MSN-Pyr). These mixtures were mechanically stirred during 1h at 40°C. Then, were added 1.75 mL of NaOH solution (1.6M) and after 15 minutes 2.5 mL of TEOS were added dropwise. The solutions were left stirring for, at least, 3 hours (Figure 15). The mesoporous nanoparticles were recovered by centrifugation at 80000 x g for 15 minutes at 20°C and were washed two times with a mixture of ethanol and water (50% v/v) and one time with absolute ethanol, discarding each time the supernatant. The MSNs were dried at 60°C overnight a ventilated oven (Figure 16).

In the case of the synthesis with the fluorinated surfactant (HFDePC), 0.875 mL of a 4.8 M NaCl solution was added to increase the particle size in order to allow an analysis of these particles in TEM.

To study the effect of the ratio between TEOS concentration and fluorinated surfactant concentration, it was made a synthesis in which was added 10 times more volume of TEOS, the other parameters remained equal.

Figure 15: Synthesis of 1-MSNs-Pyr, 1-MSNs-HFDePC and 1-MSNs-Met, respectively.

Figure 16: 1-MSNs-Pyr, 1-MSNs-HFDePC and 1-MSNs-Met, respectively, after washing and drying.

2.3.2.2. Template removal

The template in all the MSNs were removed with various methods: solvent extraction with acidified ethanol, solvent extraction with THF in reflux, solvent extraction with DCM in reflux and

calcination. Extractions with the addition of a salt were also tried, i.e., extraction with THF at reflux and at room temperature with Lithium Bromide (LiBr).

Calcination of all 1-MSNs was performed applying a 1°C/min temperature increase rate up to 500°C at a nitrogen atmosphere, following 6 h at 600°C in an air atmosphere, with an air flow of 8 L air/g particles/h.

Solvent extraction with acidified ethanol was performed in a polypropylene flask, with an acidified ethanolic solution (0.5 M HCl, 10 mL for each 200 mg of MSNs), and stirred overnight at 50 ºC (Figure 17). Then the mixture was centrifuged at 9500 rpm for 10 minutes and washed three times with absolute ethanol. The MSNs were dried overnight at 60°C in a ventilated oven.

Figure 17: Example of an extraction with EtOH/HCl.

Solvent extraction with THF in reflux was performed in a 50 mL round-bottomed flask with 25 mL of THF and 500 mg of each sample MSNs and it was refluxed overnight at 80 ºC. Then the mixture was centrifuged at 9500 rpm for 10 minutes and washed three times with absolute ethanol. The MSNs were dried overnight at 60°C in a ventilated oven.

Solvent extraction with DCM in reflux was performed in a 50 mL round-bottomed flask with 25 mL of THF and 500 mg of each sample MSNs and it was refluxed overnight at 45 ºC. Then the mixture was centrifuged at 9500 rpm for 10 minutes and washed three times with absolute ethanol. The MSNs were dried overnight at 60°C in a ventilated oven.

The extractions with THF and LiBr were made with 12.5 mL of a solution of 0.5 M LiBr in THF along with 250 mg of MSNs in a 50 mL round-bottomed flask. One was made at reflux temperature and the other at room temperature. Then both mixtures were centrifuged at 9500 rpm for 10 minutes and washed three times with absolute ethanol. The MSNs were dried overnight at 60°C in a ventilated oven.

2.3.3. Synthesis of Double Template MSNs (2-MSNs)

2-MSNs were synthesized by the same method as 1-MSNs, that is, by the modified Stöber method, differing only in the fact that two surfactants were added instead of one. In a 500 mL polypropylene flask, 240 mL of deionized (DI) water and the two surfactants were added. Two syntheses were performed with 771 mg of HFDePC and 500 mg of CTAB. These mixtures were mechanically stirred during 1h at 40°C. Then, were added 1.75 mL of NaOH solution (1.6M) in one of the mixtures and in the other mixture were added 1.75mL of the same NaOH solution and 0.875 mL of NaCl (4.8M), and after 15 minutes 2.5 mL of TEOS were added dropwise. The solutions were left stirring for, at least, 3 hours. The mesoporous nanoparticles were recovered by centrifugation at 80000 x g for 15 minutes at 20°C and were washed two times with a mixture of ethanol and water (50% v/v) and one time with absolute ethanol, discarding each time the supernatant. The MSNs were dried at 60°C overnight a ventilated oven.

3. Results and Discussion

The aim of this novel project was to develop a hybrid nanocontainer based on mesoporous silica nanoparticles with a double pore system. The study was based on four surfactants with different characteristics, hexadecyltrimethylammonium bromide (CTAB), 1-hexadecyl-3-methylimidazolium chloride (Met), 1-hexadecylpyridinium chloride (Pyr) and 1H1H2H2H-perfluorodecylpyridinium chloride (HFDePC), in order to obtain a system with a double pore system in which both templates are selectively removed. For this, syntheses of single templated nanoparticles were performed and then, several template extraction methods were studied, in order to determine the best pair of surfactants for selective extraction (Figure 10).

3.1. Synthesis and Characterization of Single Template MSNs (1-MSNs)

In order to determine the best pair of surfactants to use in the synthesis of MSNs with two pore systems, independent syntheses were made with CTAB and three new templates: 1-hexadecyl-3-methylimidazolium chloride (Met), 1-hexadecylpyridinium chloride (Pyr) and 1H1H2H2H-perfluorodecylpyridinium chloride (HFDePC), where the first two are ionic liquids and the last is a fluorinated surfactant. The syntheses were performed under the same conditions for all surfactants, with a 5.7 mM concentration for all of them. Syntheses were performed with CTAB to serve as a reference. Table 1 presents a summary of synthesis details concerning each template, including their CMC.

Table 1: Quantities of surfactants for each synthesis and respective CMC.

Surfactant	Molecular Weight (g/mol)	Quantity (mg) (5.7 mM concentration)	CMC (mM)
CTAB	364.5	500	0.92 – 1.0[61,62]
Met	343	471	1.0[63]
Pyr	340	466	0.9[64]
HFDePC	561.7	771	2.5[60]

The synthesis of 1-MSNs starts by mixing the template with water, which is stabilized at the same temperature (40°C) for about an hour, then the base is added, in this case NaOH and, finally, TEOS is added drop by drop. The synthesis is completed after 3 hours. The same concentration of NaOH was used in all syntheses (1.6 M) to analyze the differences in sizes at the end. As mentioned in section 1.2.3, the NaOH concentration dictates the size of the final particles, i.e., the higher the concentration, the larger the particles and vice versa. This is due to the fact that there are more OH^-

groups that interact with the positive charges on the micelle surface, which decreases their stability and, therefore, aggregates to form larger particles.

3.1.1. Nanoparticle Morphology

Before removing the template, the diameter distributions of the 1-MSNs were determined by TEM. Samples of MSNs with CTAB (1-MSNs-C), with Met (1-MSNs-Met), with Pyr (1-MSNs-Pyr) and with HFDePC (1-MSNs-HFDePC), were analyzed.

In Figure 18 to Figure 25 are show the TEM images of each sample and their respective size distribution. The mean diameters obtained were: 69 ± 6 nm for 1-MSNs-C, 73 ± 10 nm for 1-MSNs-Met, 64 ± 9 nm for 1-MSNs-Pyr, 21 ± 2 nm for 1-MSNs-HFDePC, 61 ± 10 nm for 1-MSNs-HFDePC-NaCl and 17 ± 3 nm for 1-MSNs-HFDePC(+TEOS).

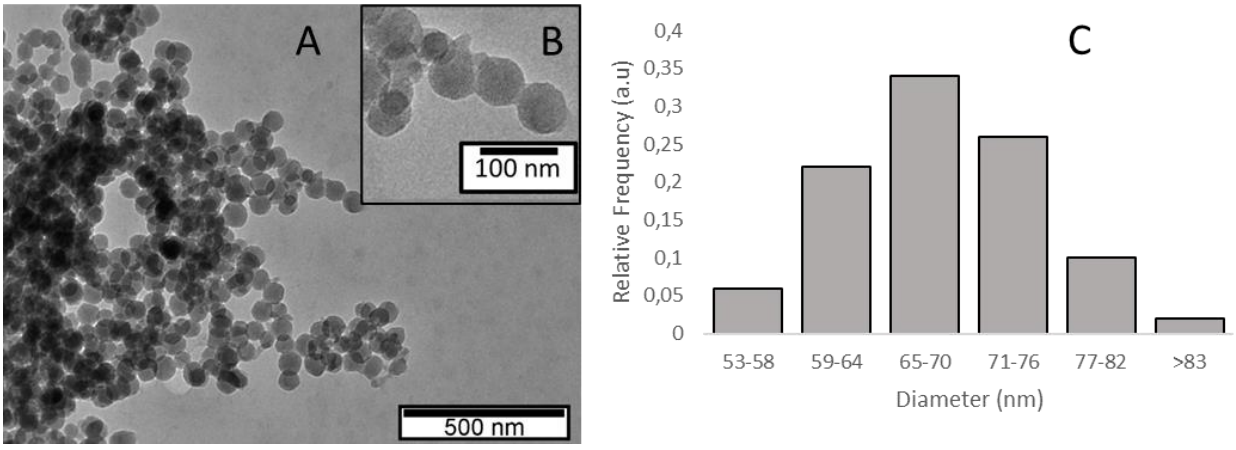

Figure 18: TEM images of sample 1-MSNs-C: A - 500 nm scale; B-100 nm scale, and respective size distribution (C). Mean diameter: 69 ± 6 nm.

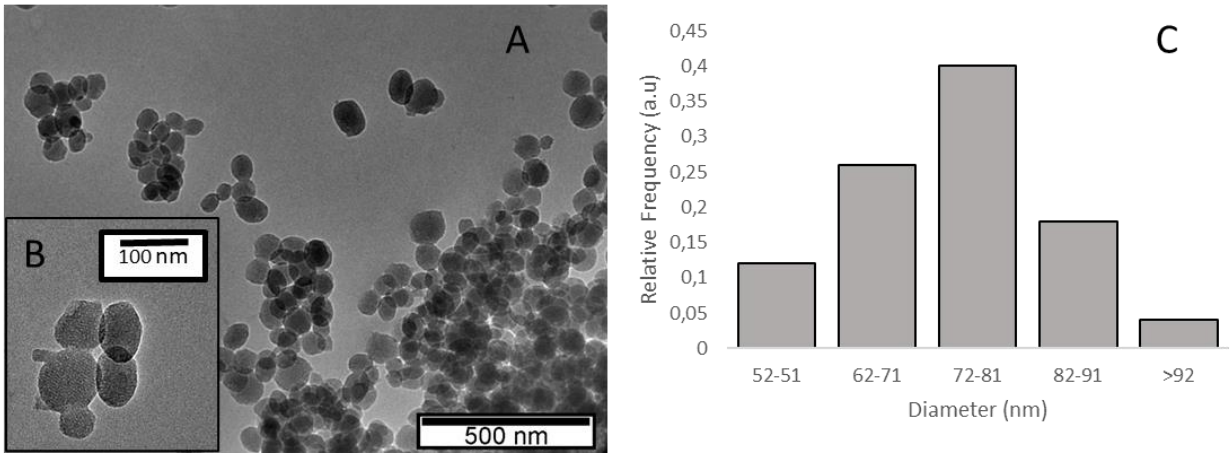

Figure 19:TEM images of sample 1-MSNs-Met: A - 500 nm scale; B-100 nm scale, and respective size distribution (C). Mean diameter: 73± 10 nm.

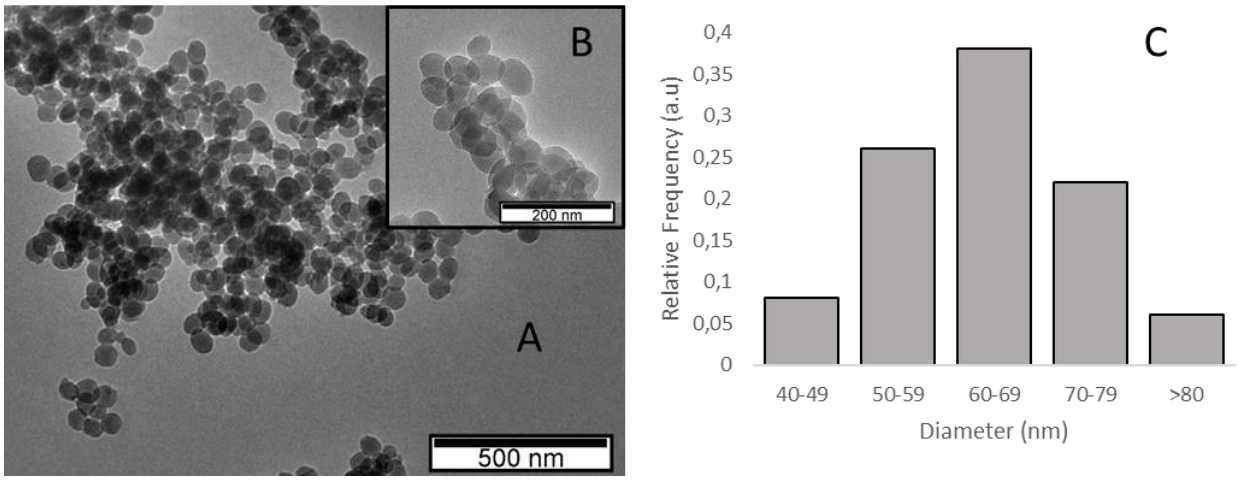

Figure 20:TEM images of sample 1-MSNs-Pyr: A - 500 nm scale; B-200 nm scale, and respective size distribution (C). Mean diameter: 64 ± 9 nm.

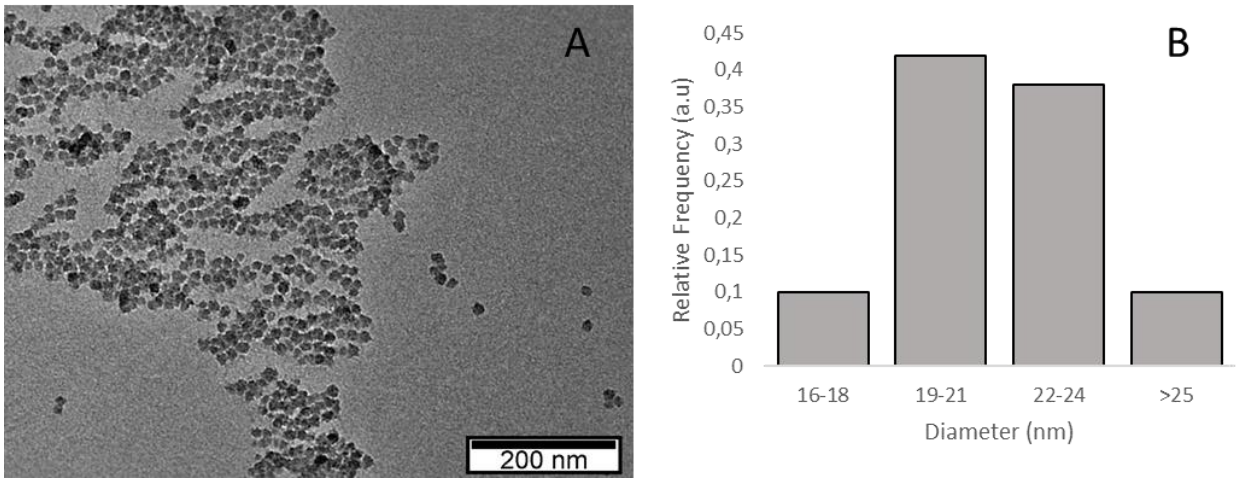

Figure 21: TEM images of sample 1-MSNs-HFDePC: A - 500 nm scale and respective size distribution (B). Mean diameter: 21 ± 2 nm.

As we can see, in samples 1-MSNs-C, 1-MSNs-Met and 1-MSNs-Pyr, Figure 18, Figure 19 and Figure 20, the size distribution is similar with low dispersity and their pore system is well defined, that is, the pores are more well packed. All of these three surfactants have a hydrocarbon chain of sixteen carbons, so the only difference between them is the cation, which do not influence the mean size of particles, since they all have similar diameters. In the fluorinated sample (Figure 21) the particles obtained were too small to see the pore system in TEM. The reason for this could be that the micelles are very stable, which leads to many points of nucleation of small size, i.e., due to its stability there is no aggregation. In order to increase the diameter, a solution of NaCl 4.8 M was added to the synthesis. The addition of salt decreases the colloidal stability due to the charge screening at the micelle surface (at higher ionic strength).[13] This sample was named of 1-MSNs-HFDePC-NaCl (Figure 22). The mean diameter obtained was 61 ± 10 nm.

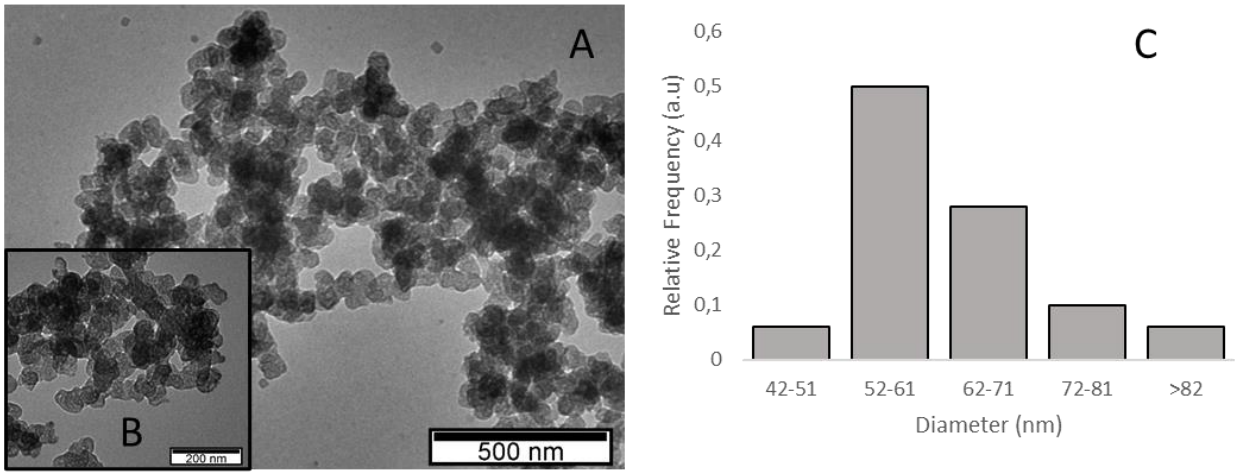

Figure 22:TEM images of sample 1-MSNs-HFDePC-NaCl: A - 500 nm scale; B-200 nm scale, and respective size distribution (C). Mean diameter: 61 ± 10 nm.

After the addition of salt, larger particles were obtained, as expected, with the diameter increasing from 21 nm to 61 nm. Compared with the 1-MSNs-HFDePC sample, we observe that the shape of the MSNs of the 1-MSNs-HFDePC-NaCl sample is not completely spherical, and that the pore system is not as organized as in the 1-MSNs-C, 1-MSNs-Met and 1-MSNs-Pyr samples. Also, the pores of these nanoparticles do not appear to be hexagonally arranged (Figure 22).

A synthesis was also made with the HFDePC template with a higher concentration - 7.2 mM. The CMC of HFDePC is higher than the CMC of the other surfactants, which are around 1mM, so in order to obtain approximately the same quantity of micelles we increase the concentration of the fluorinated surfactant in the synthesis. The initial concentration (5.7 mM) was selected to be 4.7mM higher than the CMC of CTAB, Met and Pyr, therefore we used a concentration of 7.2 mM of fluorinated surfactant (also 4.7 mM higher than its CMC). The resulting nanoparticles are shown in Figure 23. The particles obtained are not spherical: there are particles with an oblong shape and some larger agglomerates. Therefore, it is not possible to determine the diameter of these NPs. However, it is possible to see that the particles are porous.

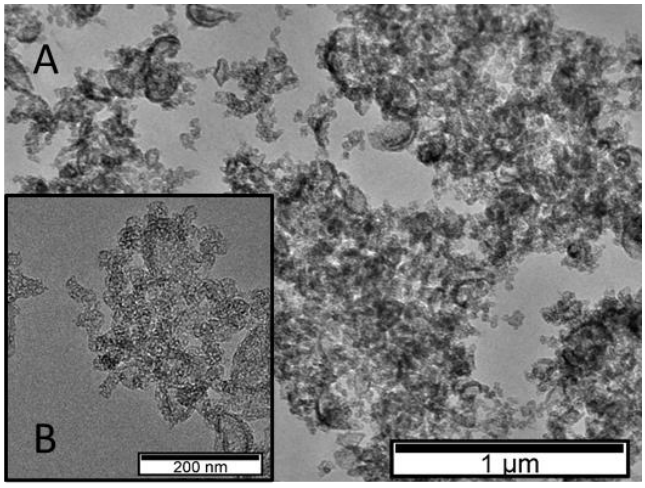

Figure 23: TEM images of sample 1-MSNs-HFDePC (7.2 mM): A - 1 µm scale; B-200 nm scale.

According to the literature, the HFDePC surfactant leads to different particle shapes and pore arrangements when different ratios of TEOS and fluorinated surfactant concentrations are used. The larger the ratio between the concentration of TEOS and HFDePC, the rounder the particles will be and the pore structure will have more order. Therefore, a synthesis was performed using a quantity of TEOS 10 times higher for the same concentration of fluorinated surfactant (5.7 mM) which increased the concentration ratio by 10 times. [65,66] As expected, we obtained more particles, due to the fact that it was used much more surfactant and, therefore, it was formed more micelles. Because of this there are more active centers for TEOS-template interaction and so more particles can be formed. The results for this sample, 1-MSNs-HFDePC(+TEOS) are shown in Figure 24. The mean diameter obtained was 17 ± 3 nm.

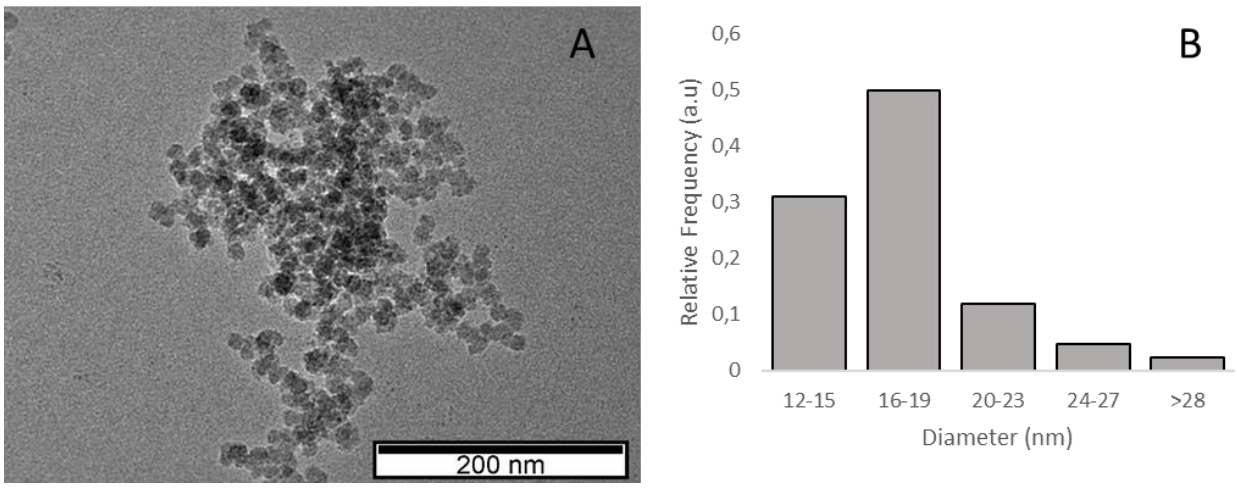

Figure 24: TEM images of sample 1-MSNs-HFDePC(+TEOS): A - 200 nm scale and respective size distribution (B). Mean diameter: 17 ± 3 nm.

As in the 1-MSNs-HFDePC sample (Figure 21) the NPs are too small to see if the pores are ordered or even if there are pores. Therefore, the same approach as before was used, an addition of a 4.8 M NaCl solution during the synthesis, to increase the particle size, allowing the visualization of the pores. The resulting NPs (1-MSNs-HFDePC(+TEOS)-NaCl) are shown in Figure 25.

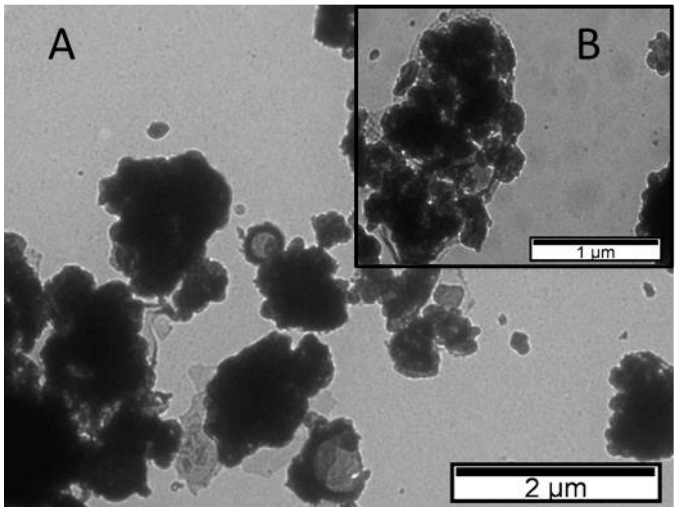

Figure 25: TEM images of sample 1-MSNs-HFDePC(+TEOS)-NaCl: A - 2 µm scale; B- 1 µm scale.

As we can see, very large agglomerates of particles were obtained with some vesicle-like hollow silica particles. It is possible to observe in Figure 25B that the particles are more elongated. This could mean that too much NaCl was used or that the TEOS/HFDePC concentration ratio was too low. In the literature[65], it is reported that samples with a TEOS/HFDePC concentration ratio between 30 and 170 have vesicle-like particles and are more elongated, so since our sample have a ratio of 82, these results

are in agreement. In order to obtain rounder particles, the concentration ratio should be increased. As the particles are very agglomerated, it is not possible to determine their diameter or their size distribution.

The mean diameter of each sample obtained by TEM is present in Table 2. We can see that 1-MSNs-C, 1-MSNs-Met and 1-MSNs-Pyr are all the same size. In these three templates, the only difference is the cation since they have the same aliphatic chain, so we can conclude that the cation has no influence on the size of the nanoparticles. When the hydrophobic part is not the same, we can see that the diameter changes, i.e., when using a fluorinated surfactant (1-MSNs-HFDePC) the micelles formed are very stable which leads to many points of nucleation of small size, i.e., due to its stability there is less micelle aggregation with smaller micelle bundles, leading to smaller particles. It is possible to conclude that when adding NaCl, the colloidal stability decreases due to charge screening at the surface of the micelles, therefore the nanoparticles were obtained with a bigger diameter. Finally, when using more TEOS, more nanoparticles are formed but because the micelles are too stable, like the initial sample 1-MSNs-HFDePC, they have a small size too.

Table 2: Particles' mean diameter of each sample obtained by TEM and respective standard deviation.

Sample	D_{TEM} (nm)
1-MSNs-C	69 ± 6
1-MSNs-Met	73 ± 10
1-MSNs-Pyr	64 ± 10
1-MSNs-HFDePC	21 ± 2
1-MSNs-HFDePC-NaCl	61 ± 10
1-MSNs-HFDePC(+TEOS)	17±3

3.1.2. Template Removal and Porosity Characterization

The main goal is to be able to remove the templates selectively, i.e., solvents must be found that remove one template but not the other. One of the most important factors for an effective template removal is its solubility in the solvent used, since it facilitates its removal from the pores. Therefore we tested the solubility of the four surfactants, CTAB, Met, Pyr e HFDePC, in various solvents.[38,39] The solvents were chosen in order to comprise most of the solvent families, i.e., ethers, alkanes, chlorinated chains, alcohols, etc. Thus, four solvents were tested, THF, hexane, dichloromethane (DCM) and EtOH. The results obtained are shown in Table 3. The surfactants are soluble in the solvent if they dissolve in it.

Table 3: Surfactants' solubility in THF, Hexane, DCM and EtOH. S=Soluble; NS=Not Soluble.

Surfactant	THF	Hexane	DCM	EtOH
CTAB	NS	NS	S	S
Met	S	NS	S	S
Pyr	NS	NS	S	S
HFDePC	NS	NS	NS	NS

As we can see the surfactants are all non-soluble in hexane, so this solvent is excluded. THF, DCM and EtOH may have selectivity in removing templates since there is no solubility or insolubility in all of them. Thus, the removal of the four surfactants was tested with acidified EtOH, refluxing THF and refluxing DCM. Removal by calcination was also carried, where all template is removed and can be used as control to evaluate the extractions efficiency with the different solvents.

Empirically, it can be seen if there was template removal if the mass obtained after the extraction is lower when compared with the initial mass. However, the precise data must be obtained by nitrogen adsorption. In all of the studies were used 500 mg of each set of particles as initial mass, except in calcination and in the extraction of 1-MSNs-HFDePC-NaCl with EtOH/HCl, where we used 300 mg. The results are shown in Table 4 and Table 5.

Table 4: Weight loss after template removal by THF, DCM and acidified EtOH.

Solvent	THF	DCM	EtOH/HCl
	Weight Loss (%)		
1-MSNs-C	20	14	62
1-MSNs-Met	18	12	72
1-MSNs-Pyr	27	13	67
1-MSNs-HFDePC	27	24	43
1-MSNs-HFDePC-NaCl	--------	--------	39

Table 5: Initial and final masses of NPs after template removal by calcination.

Calcination

	Initial Mass (mg)	Final Mass (mg)	Weight Loss (%)
1-MSNs-C	500	241	52
1-MSNs-Met	416	200	52
1-MSNs-Pyr	430	240	44
1-MSNs-HFDePC	278	180	35
1-MSNs-HFDePC-NaCl	500	290	42

It is known that surfactant removal by calcination is the most efficient process since it removes all organic components from the silica material.[34,38,67] The results obtain by this method will be used as control for comparison, in order to check the washing with EtOH/HCl extraction, since this method is known to also remove almost all of the existing surfactant.[67] As we can see in Table 4, comparing with the results obtained in Table 5, with THF in reflux there is a partial removal of all surfactants, so this solvent cannot be used for selective removal. With DCM extraction, as in THF extraction, there is a partial removal of all surfactants but less pronounced, i.e., it removes less and therefore this solvent cannot be used for selective removal. With acidified EtOH we can see that there is a similar removal for all surfactants, which means that it cannot perform a selective extraction. This method has a greater mass loss in relation to calcination. Since the mass loss values cannot be higher than those of calcination, we can conclude that there were losses during the procedure, probably during centrifuging and washing. The efficiency of extraction using acidified ethanol has to do with the fact that the H^+ in HCl is such a small ion that it can penetrate the pores of the NPs and therefore destabilize the ionic bond between the surfactants and the surface anionic groups of silica. With the same reasoning, one way to improve the extraction with THF is to use a salt, in this case a lithium salt, in which the Li^+ ion will play the same role as the H^+ ion. Template removal with THF and lithium bromide (LiBr, 0.5 M) was made in 1-MSNs-C, in reflux and at room temperature. The results are shown in Table 6.

Table 6: Final masses of 1-MSN-C NPs after template removal by THF with LiBr at different temperatures.

1-MSN-C NPs Extraction with THF and LiBr

	Reflux	Room Temperature
Initial Mass (mg)	250	268
Final Mass (mg)	161	182
Weight Loss (%)	36	32

As expected, the weight loss increases when a salt is used, which confirms the previous hypothesis. However, the values obtained did not come close to the mass loss values obtained in the extraction with EtOH/HCl.

The results obtained between different surfactants extracted with the same method, were compared using the number of moles of surfactant lost per gram of particle used in the extraction (Table 7).

Table 7: Surfactant Loss (mmol)/g particles after template removal by THF, DCM and acidified EtOH.

Solvent	THF	DCM	EtOH/HCl
	Surfactant Loss (mmol)/g particles		
1-MSNs-C	0.55	0.40	1.70
1-MSNs-Met	0.53	0.34	2.10
1-MSNs-Pyr	0.79	0.37	1.98
1-MSNs-HFDePC	0.48	0.42	0.77
1-MSNs-HFDePC-NaCl	--------	--------	0.69

When using THF, we can see that all the surfactants are similarly removed. However, 1-MSNs-Pyr shows larger removal than the others, which may suggest a selective extraction method. It is, however not very efficient due to the difference not being very accentuated. In the extraction with DCM, we can conclude that the removal of each surfactant is very similar, so there is no selective removal of any surfactant. With EtOH/HCl, the removal is more efficient in 1-MSNs-C, 1-MSNs-Met and 1-MSNs-Pyr, as it removes more than twice as much as in 1-MSNs-HFDePC, and, therefore, it can be considered a selective method to this surfactant (again, it may not be very efficient since the variation is not very large). It should be noted that the HFDePC surfactant is the least removed with EtOH/HCl, which may suggest that it is not as easy to remove as the remaining surfactants, even with the most effective method.

To confirm the results obtained above, it is necessary to compare them with the results obtained by nitrogen adsorption, that is, by the BET (Brunauer-Emmett-Teller) and BJH (Barrett-Joyer- Halenda) method, in which the surface area is obtained in the first, and the pore volume and pore diameter in the second. Both in BET and in BJH methods, nitrogen is usually used because of its high purity and strong interaction with most solids. [42–44]

The materials prepared in this project typically present mesopores, so the most likely isotherm will be of type IV. Nitrogen adsorptions were performed for 1-MSNs-C, 1-MSNs-Met, 1-MSNs-Pyr and 1-MSN-HFDePC, extracted with EtOH/HCl, THF and calcinated, to obtain the specific surface area (S_{BET}), the pore volume (V_p) and the pore diameter (D_p).

The results for 1-MSNs-C are shown in Figure 26 and Table 8. As expected, both extractions with EtOH/HCl and calcination yield type IV isotherms, which means that practically all surfactant are removed. However, the THF extraction is a type IV isotherm but very little accentuated, which suggests that not all surfactant was removed. These conclusions are supported by the results shown in Table 8 since the BET surface area, the pore volume and the pore diameter are significantly higher in both calcination and extraction with EtOH/HCl compared to extraction with THF. The extraction with THF is therefore less efficient than extraction with EtOH/HCl or calcination, as concluded earlier by the study of mass loss after the extraction. That said, it is possible to confirm that the smaller the mass loss, the less surfactant was extracted by the method. The different values of calcination and extraction with EtOH/HCl derive from the condensation and contraction of the silica structure when submitted to high temperatures.

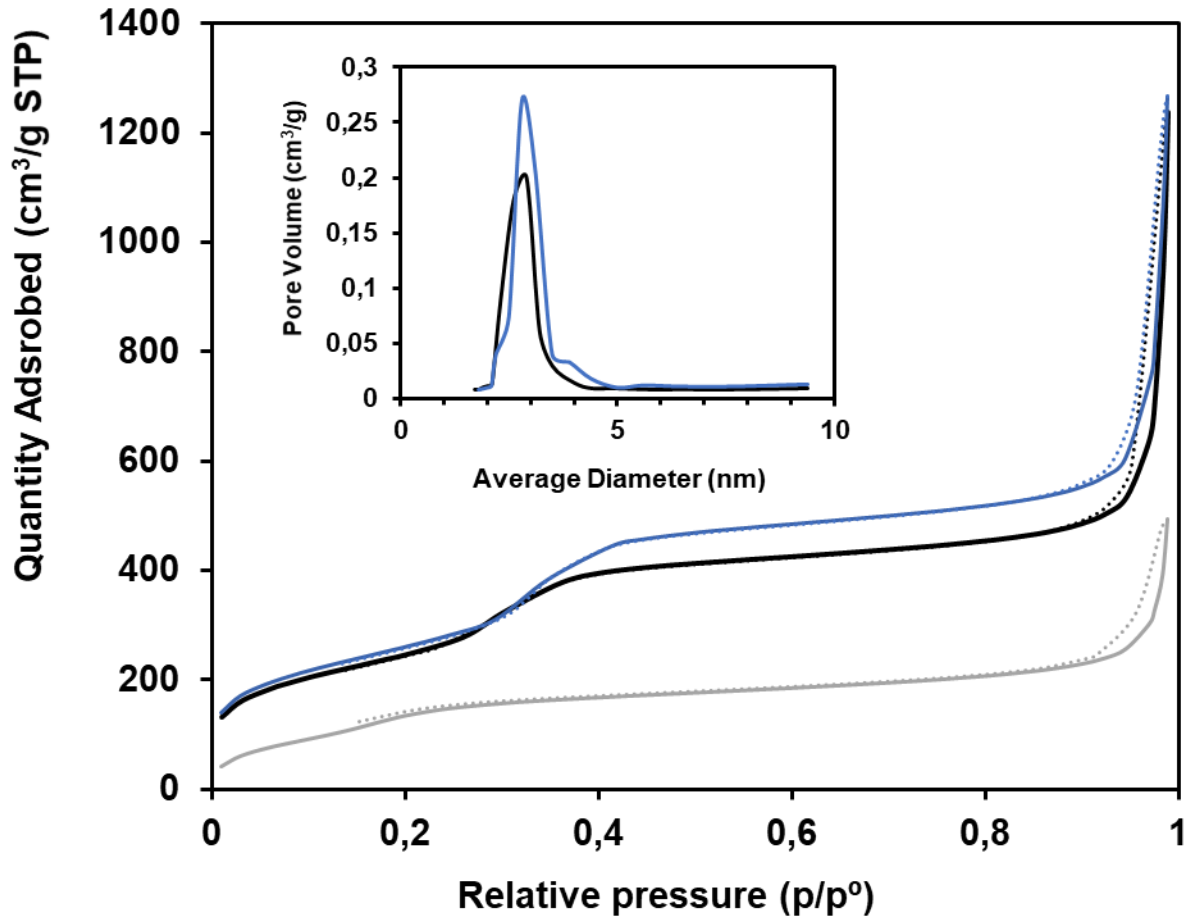

Figure 26: Nitrogen adsorption (solid line)-desorption (dotted line) isotherms for 1-MSNs-C calcinated (black), extracted with EtOH/HCl (blue) and with THF (grey) and corresponding pore size distribution (inset).

Table 8: Results obtained for 1-MSNs-C by nitrogen adsorption.

	S_{BET} (m^2/g)	V_p(cm^3/g)	D_p (nm)
1-MSNs-C Calcination	900	0.7	2.9
1-MSNs-C EtOH/HCl	950	0.8	2.8
1-MSNs-C THF	570	0.33	2.7

The results for 1-MSNs-Met are shown in Figure 27 and Table 9. As we can see, the nitrogen adsorption results for 1-MSNs-Met are very similar to the results for 1-MSNs-C and so, the same conclusions can be drawn. We can see in Figure 27 that both extractions with EtOH/HCl and calcination are type IV isotherms but in the extraction with THF the isotherm is a type IV isotherm but very little accentuated, because the surfactant was not all removed by this last extraction method, as in the extractions of 1-MSNs-C. Analyzing Table 9, we can confirm that much more surfactant is removed with calcination and extraction with EtOH/HCl than with extraction with THF, although the latter has removed a little more surfactant than in 1-MSNs-C. Once again, the empirical study of mass loss is correct.

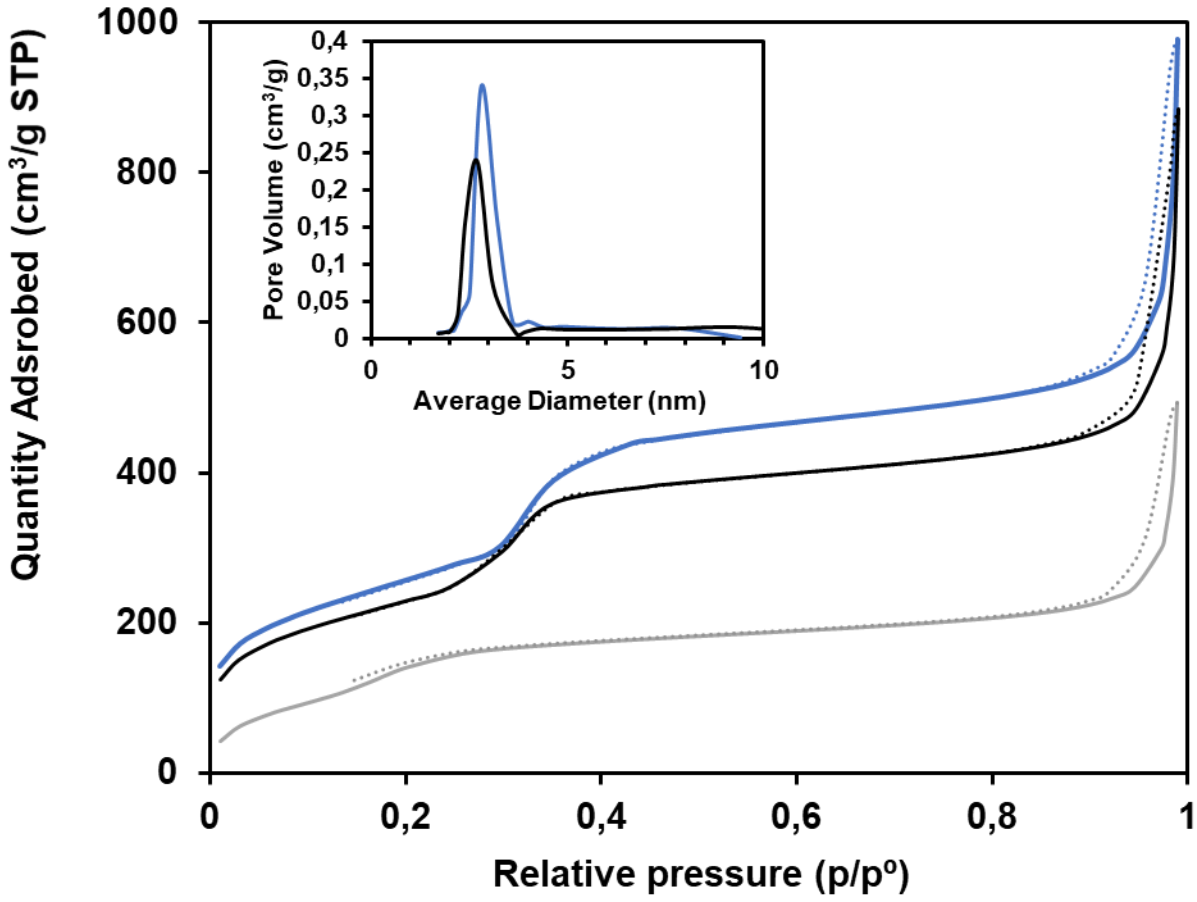

Figure 27: Nitrogen adsorption (solid line)-desorption (dotted line) isotherms for 1-MSNs-Met calcinated (black), extracted with EtOH/HCl (blue) and with THF (grey) and corresponding pore size distribution (inset).

Table 9: Results obtained for 1-MSNs-Met by nitrogen adsorption.

	S_{BET} (m^2/g)	V_p(cm^3/g)	D_p (nm)
1-MSNs-Met Calcination	840	0.62	2.7
1-MSNs-Met EtOH/HCl	940	0.75	2.8
1-MSNs-Met THF	600	0.32	2.5

The results for 1-MSNs-Pyr are shown in Figure 28 and Table 10. Again, the same conclusions can be drawn as in the two adsorptions above, extraction with EtOH/HCl and calcination removes more surfactant than extraction with THF. However, in the extraction with THF we can see that more surfactant is removed in 1-MSNs-Pyr than in 1-MSNs-C and 1-MSNs-Met. Once again, these results confirm the empirical study of the weight loss we can conclude that those results are congruent with these ones.

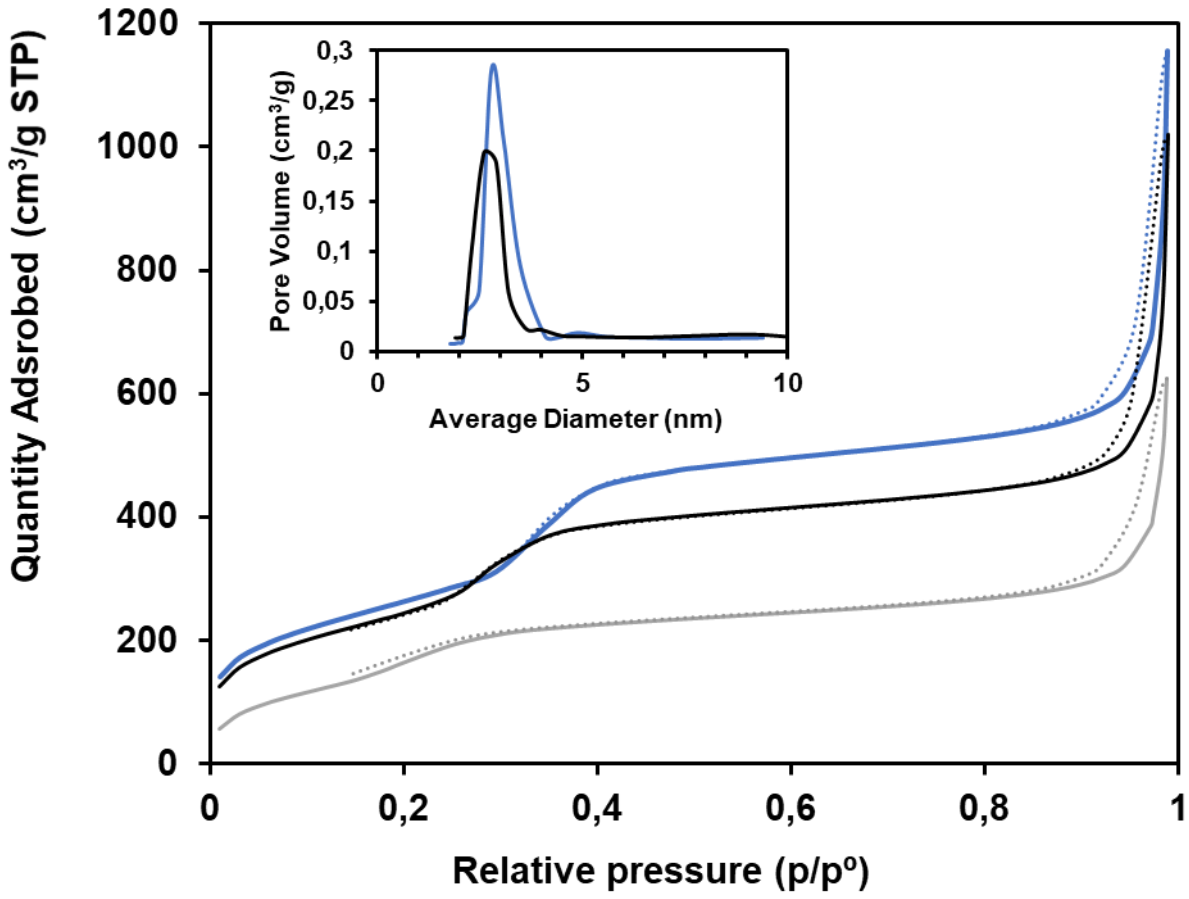

Figure 28: Nitrogen adsorption (solid line)-desorption (dotted line) isotherms for 1-MSNs-Pyr calcinated (black), extracted with EtOH/HCl (blue) and with THF (grey) and corresponding pore size distribution (inset).

Table 10: Results obtained for 1-MSNs-Pyr by nitrogen adsorption.

	S_{BET} (m^2/g)	V_p(cm^3/g)	D_p (nm)
1-MSNs-Pyr Calcination	900	0.75	2.7
1-MSNs-Pyr EtOH/HCl	970	0.80	2.8
1-MSNs-Pyr THF	650	0.42	2.6

Finally, the results for 1-MSNs-HFDePC are shown in Figure 29 and Table 11. Here, the isotherms are a little different from the isotherms of the previous particles, most notably in the fact that the adsorption and desorption isotherms are not very coincident. The extractions with EtOH/HCl and THF are type IV isotherms. However, for 1-MSNs-HFDePC and 1-MSNs-HFDePC-NaCl calcinations, the isotherms are a type IV but very little accentuated, they are almost a type II isotherm, which suggests that not all surfactant was removed and that the pore structure collapsed, probably due to the high temperatures during calcination. These conclusions are supported with the results shown in Table 11, since the BET surface area and the pore volume are significantly higher in both EtOH/HCl and THF extractions. It can be confirmed that calcinations, when using this template, are not the best extraction method since the values obtained in Table 11 are very low. Comparing the THF extraction and EtOH/HCl extraction results to the mass loss study, since these methods were the only ones that did not collapse, the second method removed more surfactant in both studies.

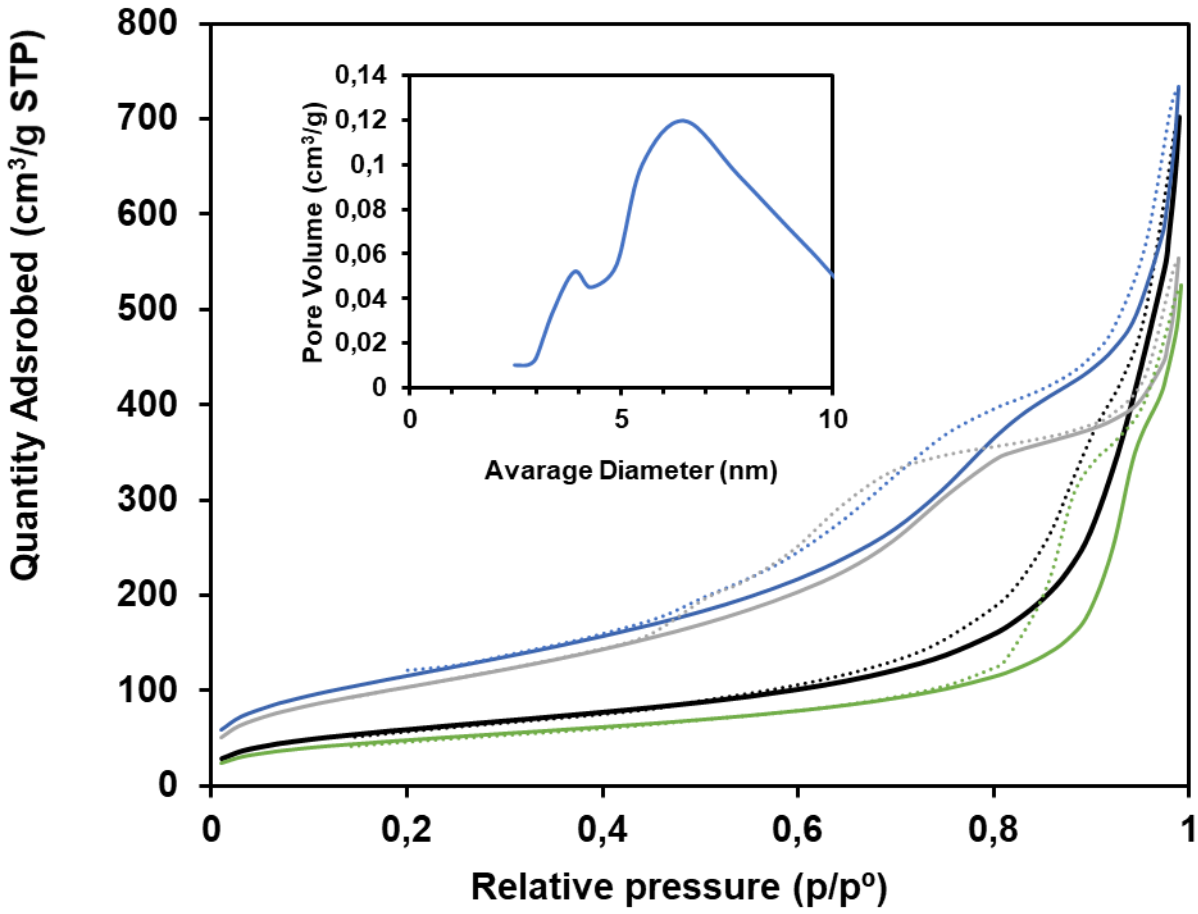

Figure 29: Nitrogen adsorption (solid line)-desorption (dotted line) isotherms for 1-MSNs-HFDePC calcinated (black), extracted with EtOH/HCl (blue), with THF (grey) and for 1-MSNs-HFDePC-NaCl calcinated (green) and corresponding pore size distribution (inset).

Table 11: Results obtained for 1-MSNs-HFDePC and 1-MSNs-HFDePC-NaCl by nitrogen adsorption.

	S_{BET} (m^2/g)	V_p(cm^3/g)
1-MSNs-HFDePC Calcination	220	0.72
1-MSNs-HFDePC-NaCl Calcination	175	0.70
1-MSNs-HFDePC EtOH/HCl	430	0.71
1-MSNs-HFDePC THF	390	0.62

As all the results of the nitrogen adsorptions are in agreement with the empirical results of the mass loss study after the extraction, it can be concluded that the extractions with DCM would have results very similar to those of THF, that is, smaller surface areas and smaller pore volume, so it is an

inefficient extraction method for all surfactants, which means that with this solvent it is not possible to do a selective extraction of templates. In the extraction with THF with LiBr (mass loss analysis) we know that there was higher removal when compared with pure THF, so we would expect that the results of the adsorption of this method would be better, that is, the nanoparticles would have a greater surface area and a larger pore volume, making it a more efficient method. We can also conclude that none of the studied extraction methods can selectively remove one of the surfactants efficiently, since there are no significant differences in the different nanoparticles extracted by the same method.

3.2. Synthesis and Characterization of Double Template MSNs (2-MSNs)

Two syntheses were performed with a dual system of templates, HFDePC and CTAB, since these are the ones that differ the most in their molecular structure among the studied surfactants and, therefore, they have the largest probability of not forming mixed micelles and also of being selectively extracted. The syntheses were done with the same amounts of all components as the 1-MSNs. The only difference is the use of two surfactants, which are added with the same mass as in 1-MSNs. The only difference between the experiments was the addition of a NaCl solution in one of them (2-MSNs-C-HFDePC-NaCl), to evaluate the effect of this salt in syntheses with a double pore system. These experiments were named 2-MSNs-C-HFDePC and 2-MSNs-C-HFDePC-NaCl.

From the two syntheses made, a much lower final mass was obtained in the synthesis in which NaCl was not added. This is probably because NaCl increases the size of the particles (increasing the ionic strength, there is a destabilization of the micelles, causing aggregation and therefore larger particles). We obtained 100 mg of 2-MSNs-C-HFDePC and 410 mg of 2-MSNs-C-HFDePC-NaCl. The amount of TEOS added in both syntheses was not increased, so it was expected that the mass obtained would not be very high, since even if a large number of micelles were formed, if there are no silica precursor, no particles will form. Therefore, the solution is to increase the volume of TEOS added to the syntheses in order to get more particles. To determine the mean diameter of the nanoparticles obtained by this method, their size distributions were analyzed by TEM.

The results obtained by TEM for samples 2-MSNs-C-HFDePC and 2-MSNs-C-HFDePC-NaCl are shown in Figure 30 and Figure 31, respectively, and the mean diameter of each sample obtained by TEM is present in Table 12

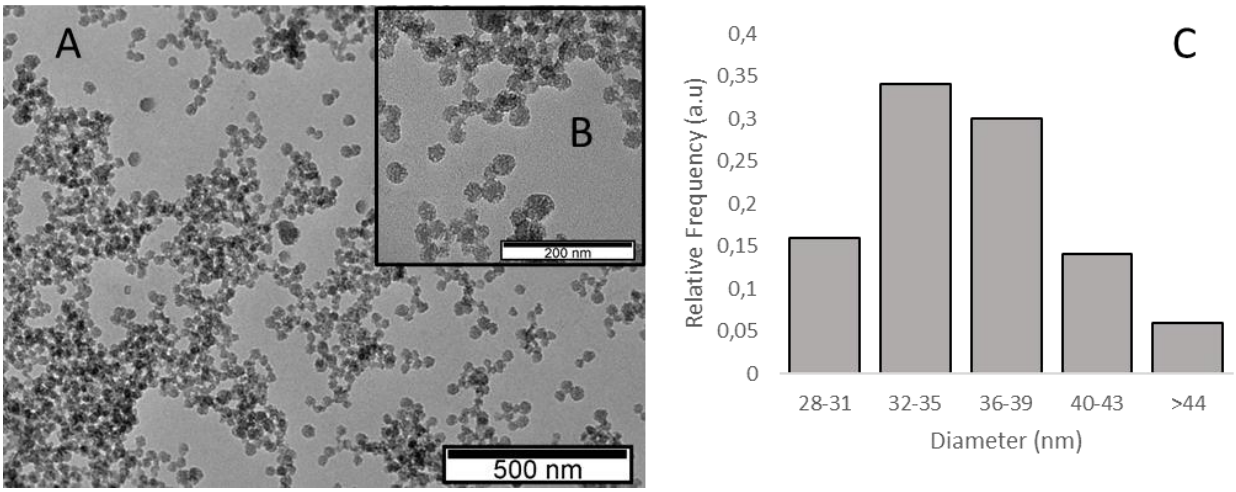

Figure 30: TEM images of sample 2-MSNs-C-HFDePC: A - 500 nm scale; B-200 nm scale, and respective size distribution (C). Mean diameter: 35 ± 4 nm.

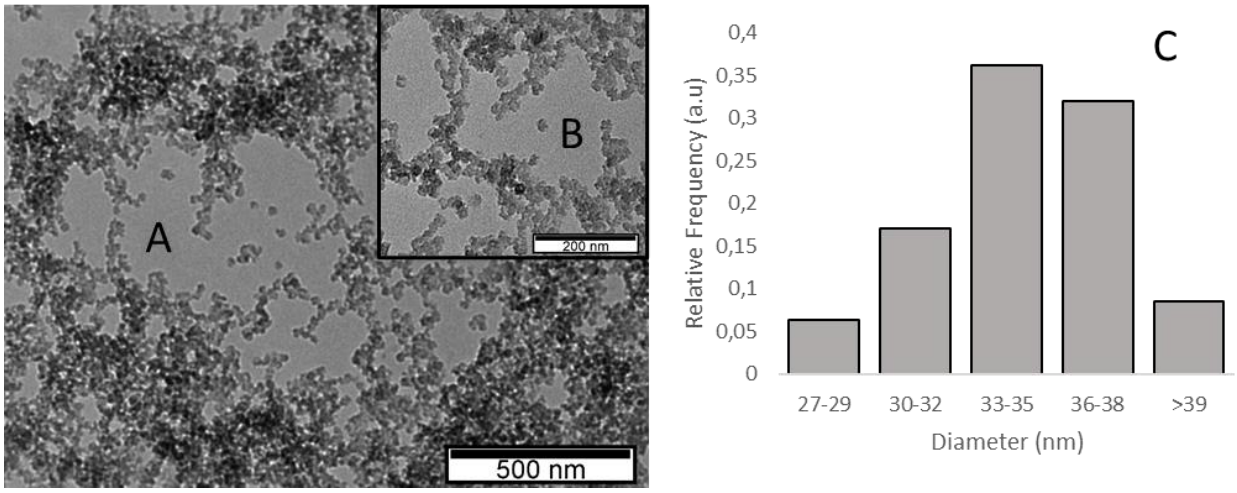

Figure 31: TEM images of sample 2-MSNs-C-HFDePC-NaCl: A - 500 nm scale; B-200 nm scale, and respective size distribution (C). Mean diameter: 34 ± 3nm.

Table 12: 2-MSNs nanoparticles mean diameter obtained by TEM and respective standard deviation.

Sample	D_{TEM} (nm)
2-MSNs-C-HFDePC	35 ± 4
2-MSNs-C-HFDePC-NaCl	34 ± 3

As we can see in Table 12, the particle diameters of the two samples are the same, which may suggest that the quantity of NaCl used was too small. However, analyzing Figure 30 and Figure 31 it is possible to see some differences. The particles in the sample 2-MSNs-C-HFDePC are rounder and appear to have more cylindrical, visible pores (with what appear to be larger-than-normal pores, visible in Figure 30B). The particles from sample 2-MSNs-C-HFDePC-NaCl appear to be less round and with a more disorganized pore system. All this can be explained by the fact that the salt (NaCl) causes electrostatic screening of the micelles surface charge, i.e., there will be a decrease in intermicellar repulsion, which affects packing of the micelles, leading to a different pore morphology in the final nanoparticles.[13]

4. Conclusions and Future Perspectives

The aim of this project was to develop a novel hybrid nanocontainer, based on mesoporous silica nanoparticles with a double pore system for selective release control. To make this possible, four surfactants, CTAB, Met, Pyr and HFDePC, were tested in the synthesis of mesoporous silica nanoparticles with a single pore system, and then their removal was evaluated by different methods: calcination, extraction with EtOH/HCl, with pure THF, with THF and LIBr and with DCM, in order to select a pair of templates for the preparation of MSNs with a double pore system.

The nanoparticles (1-MSNs-C, 1-MSNs-Met, 1-MSNs-Pyr and 1-MSNs-HFDePC) were all synthetized under the same conditions, 5.7 mM of surfactant, by the modified Stöber method and were analyzed by TEM. For 1-MSNs-C, 1-MSNs-Met and 1-MSNs-Pyr the mean diameter was very similar, 69 ± 6 nm, 73 ± 10 nm and 64 ± 9 nm, respectively, as well as the pore diameters obtained by BET. For 1-MSNs-HFDePC, the mean diameter was very small when compared to the others, 21 ± 2 nm, from which it is concluded that the micelles formed are very stable which leads to many points of nucleation of small size, i.e., due to its stability there is no aggregation, leading to a smaller sized particle. In order to increase the size of these particles several hypotheses were tested: addition of NaCl during synthesis (1-MSNs-HFDePC-NaCl), increasing HFDePC concentration to 7.2 mM (1-MSNs-HFDePC(7.2 mM)), addition of more quantity of TEOS during synthesis (1-MSNs-HFDePC(+TEOS)) and finally, addition of more TEOS and NaCl during synthesis (1-MSNs-HFDePC(+TEOS)-NaCl). The expected increase in size was obtained in 1-MSNs-HFDePC-NaCl, with a diameter of 61 ± 10 nm. From this we can conclude that, since in the 1-MSNs-C, 1-MSNs-Met and 1-MSNs-Pyr samples have the same aliphatic chain but with different cations, the cation does not influence the size of the nanoparticles, as opposed to the change in the aliphatic chain, in the fluorinated surfactant, which influences the final size.

The extraction processes demonstrate that none of the methods can selectively remove one of the surfactants efficiently, since in none of the studies there were a significantly difference between results. However, two methods stand out, and may be promising if studied further: THF removed more template in 1-MSNs-Pyr than in other nanoparticles, and EtOH/HCl removed less template in 1-MSNs-HFDePc when compared to other nanoparticles.

In order to test particles with a double pore system, MSNs with both CTAB and HFDePC were prepared, either with no NaCl (2-MSNs-C-HFDePC) and with NaCl (2-MSNs-C-HFDePC-NaCl). The diameters obtained were very similar, 35 ± 4 for the sample without salt and 34 ± 3 for the sample with salt.

Overall, our results are very promising for developing novel nanoparticles with a double pore system for selective cargo release.

In further studies, it would be interesting to test more surfactants that produce cylindrical templates, in order to achieve a more efficient selective extraction of different templates in the same

nanoparticles. To the same end, more solvent extraction methods should also be tested. Selection of both templates and removal methods should be guided by three criteria: i) the ability of the surfactants to form cylindrical or worm-like micelles; ii) a low tendency to for mixed micelles of both surfactants; and iii) the possibility to selectively extract each template in mild and controlled conditions.

5. References

1. Khan, I., Saeed, K. & Khan, I. Nanoparticles: Properties, applications and toxicities. *Arab. J. Chem.* **12**, 908–931 (2019).

2. Soni, S., Salhotra, A. & Suar, M. *Handbook of research on diverse applications of nanotechnology in biomedicine, chemistry, and engineering*. (Engineering Science Reference, 2015).

3. Vivero-Escoto, J. *Silica Nanoparticles: Preparation, Properties and Uses*. (Nova Science Publishers, Inc. New York, 2011).

4. Florek, J., Caillard, R. & Kleitz, F. Evaluation of mesoporous silica nanoparticles for oral drug delivery-current status and perspective of MSNs drug carriers. *Nanoscale* **9**, 15252–15277 (2017).

5. Yang, L. *et al.* Facile Synthesis of Hybrid Silica Nanoparticles Grafted with Helical Poly(phenyl isocyanide)s and Their Enantioselective Crystallization Ability. *Macromolecules* **49**, 7692–7702 (2016).

6. Mohanraj, V. J. & Chen, Y. Nanoparticles - A review. *Trop. J. Pharm. Res.* **5**, 561–573 (2007).

7. Jarvie, H., King, S. & Dobson, P. Nanoparticle. *Encyclopedia Britannica* 1–11 https://www.britannica.com/science/nanoparticle (2019). (Accessed in 2021-05-11)

8. Kurkina, T. & Balasubramanian, K. Towards in vitro molecular diagnostics using nanostructures. *Cell. Mol. Life Sci.* **69**, 373–388 (2012).

9. Yang, W., Wang, L., Mettenbrink, E. M., Deangelis, P. L. & Wilhelm, S. Nanoparticle Toxicology. *Annu. Rev. Pharmacol. Toxicol.* **61**, 269–289 (2021).

10. Schulz, A. & McDonagh, C. Intracellular sensing and cell diagnostics using fluorescent silica nanoparticles. *Soft Matter* **8**, 2579–2585 (2012).

11. Li, X., Wang, L., Fan, Y., Feng, Q. & Cui, F. Z. Biocompatibility and toxicity of nanoparticles and nanotubes. *J. Nanomater.* **2012**, (2012).

12. Jeelani, P. G., Mulay, P., Venkat, R. & Ramalingam, C. Multifaceted Application of Silica Nanoparticles. A Review. *Silicon* **12**, 1337–1354 (2020).

13. Ribeiro, T. *et al.* Silica nanocarriers with user-defined precise diameters by controlled template self-assembly. *J. Colloid Interface Sci.* **561**, 609–619 (2020).

14. Barbé, C. *et al.* Silica particles: A novel drug-delivery system. *Adv. Mater.* **16**, 1959–1966 (2004).

15. Gomes, M. C., Cunha, Â., Trindade, T. & Tomé, J. P. C. The role of surface functionalization of silica nanoparticles for bioimaging. *J. Innov. Opt. Health Sci.* **9**, 1–16 (2016).

16. Rahman, I. A. & Padavettan, V. Synthesis of Silica nanoparticles by Sol-Gel: Size-dependent properties, surface modification, and applications in silica-polymer nanocompositesa review. *J. Nanomater.* **2012**, (2012).

17. Stöber, W., Fink, A. & Bohn, E. Controlled Growth of Monodisperse Silica Spheres in the Micron Size Range. *J. Colloid Interface Sci.* **26**, 62–69 (1968).

18. Valtchev, V. & Tosheva, L. Porous nanosized particles: Preparation, properties, and applications. *Chem. Rev.* **113**, 6734–6760 (2013).

19. Singh, L. P. *et al.* Sol-Gel processing of silica nanoparticles and their applications. *Adv. Colloid Interface Sci.* **214**, 17–37 (2014).

20. Narayan, R., Nayak, U. Y., Raichur, A. M. & Garg, S. Mesoporous silica nanoparticles: A comprehensive review on synthesis and recent advances. *Pharmaceutics* **10**, 1–49 (2018).

21. Zheng, K. & Boccaccini, A. R. Sol-gel processing of bioactive glass nanoparticles: A review. *Adv. Colloid Interface Sci.* **249**, 363–373 (2017).

22. Green, D. L. *et al.* Size, volume fraction, and nucleation of Stober silica nanoparticles. *J. Colloid Interface Sci.* **266**, 346–358 (2003).

23. Wu, S. H. & Lin, H. P. Synthesis of mesoporous silica nanoparticles. *Chem. Soc. Rev.* **42**, 3862–3875 (2013).

24. Brinker, C. J. & Sherer, G. W. *Sol-gel science: The Physics and Chemistry of Sol-Gel Processing*. *Materials Chemistry and Physics* (Academic Press, Inc., 1990). doi:10.1016/0254-0584(90)90039-d.

25. P. Chiriac, A., E. Nita, L., Neamtu, I. & T. Nistor, M. Sol - Gel Technique Applied for Biomaterials Achievement. *Recent Patents Mater. Sci.* **4**, 224–237 (2012).

26. Zhou, Y. *et al.* Mesoporous silica nanoparticles for drug and gene delivery. *Acta Pharm. Sin. B* **8**, 165–177 (2018).

27. Trewyn, B. G., Slowing, I. I., Giri, S., Chen, H. T. & Lin, V. S. Y. Synthesis and functionalization of a mesoporous silica nanoparticle based on the sol-gel process and applications in controlled release. *Acc. Chem. Res.* **40**, 846–853 (2007).

28. Kresge, C. ., Leonowicz, M. E., Roth, W. J., Vartull, J. C. & Beck, J. S. Ordered mesoporous molecular sieves synthesized by a liquid-crystal template mechanism. *Nature* **359**, 710–713 (1992).

29. Hoffmann, F., Cornelius, M., Morell, J. & Fröba, M. Silica-based mesoporous organic-inorganic hybrid materials. *Angew. Chemie - Int. Ed.* **45**, 3216–3251 (2006).

30. Rodrigues, A. S., Ribeiro, T., Fernandes, F., Farinha, J. P. S. & Baleizão, C. Intrinsically fluorescent silica nanocontainers: A promising theranostic platform. *Microsc. Microanal.* **19**, 1216–1221 (2013).

31. Bharti, C., Gulati, N., Nagaich, U. & Pal, A. Mesoporous silica nanoparticles in target drug delivery system: A review. *Int. J. Pharm. Investig.* **5**, 124 (2015).

32. Khalil, R. A. & Zarari, A. H. A. Theoretical estimation of the critical packing parameter of amphiphilic self-assembled aggregates. *Appl. Surf. Sci.* **318**, 85–89 (2014).

33. Chiang, Y. D. *et al.* Controlling particle size and structural properties of mesoporous silica nanoparticles using the taguchi method. *J. Phys. Chem. C* **115**, 13158–13165 (2011).

34. Barczak, M. Template removal from mesoporous silicas using different methods as a tool for adjusting their properties. *New J. Chem.* **42**, 4182–4191 (2018).

35. Kumar, R., Chen, H. T., Escoto, J. L. V., Lin, V. S. Y. & Pruski, M. Template removal and thermal stability of organically functionalized mesoporous silica nanoparticles. *Chem. Mater.* **18**, 4319–4327 (2006).

36. Chen, L., Jiang, S., Wang, R., Zhang, Z. & Qiu, S. A novel, efficient and facile method for the template removal from mesoporous materials. *Chem. Res. Chinese Univ.* **30**, 894–899 (2014).

37. Idris, S. A. *et al.* Large pore diameter MCM-41 and its application for lead removal from aqueous media. *J. Hazard. Mater.* **185**, 898–904 (2011).

38. Jabariyan, S. & Zanjanchi, M. A. A simple and fast sonication procedure to remove surfactant templates from mesoporous MCM-41. *Ultrason. Sonochem.* **19**, 1087–1093 (2012).

39. Deekamwong, K. & Wittayakun, J. Template removal by ion-exchange extraction from siliceous MCM-41 synthesized by microwave-assisted hydrothermal method. *Microporous Mesoporous Mater.* **239**, 54–59 (2017).

40. Kecht, J. & Bein, T. Oxidative removal of template molecules and organic functionalities in mesoporous silica nanoparticles by H2O2 treatment. *Microporous Mesoporous Mater.* **116**, 123–130 (2008).

41. Gomes, W. A., Cardoso, L. A. M., Gonzaga, A. R. E., Aguiar, L. G. & Andrade, H. M. C. Influence of the extraction methods to remove organic templates from Al-MCM-41 molecular sieves. *Mater. Chem. Phys.* **93**, 133–137 (2005).

42. Brun, M., Lallemand, A., Quinson, J. F. & Eyraud, C. A new method for the simultaneous determination of the size and shape of pores: the thermoporometry. *Thermochim. Acta* **21**, 59–88 (1977).

43. Micromeritics Instrument Corporation. Effective Solutions for Material Characterization - Calculations. (2019).

44. Eurofins. Surface Area (BET) & Pore Size Determination (BJH). https://www.eag.com/techniques/phys-chem/bet-bjh/.(Accessed in 2021-10-14)

45. Brunauer, S., Emmett, P. H. & Teller, E. Adsorption of Gases in Multimolecular Layers. *J. Am. Chem. Soc.* **60**, 309–319 (1938).

46. Raja, P. M. V & Barron, A. R. *Physical Methods in Chemistry and Nano Science*. (LibreTexts, 2021). doi:10.1002/jctb.5000533702.

47. Gao, H. *et al.* Synthesis of core-shell and hollow structured dual-mesoporous silica templated by alkoxysilyl-functionalized ionic liquids and CTAB. *Mater. Lett.* **211**, 126–129 (2018).

48. Wang, X. *et al.* Transformation from single-mesoporous to dual-mesoporous organosilica nanoparticles. *Nanoscale* **9**, 6362–6369 (2017).

49. Zhao, S. *et al.* One-step synthesis of core-shell structured mesoporous silica spheres templated by protic ionic liquid and CTAB. *Mater. Lett.* **178**, 35–38 (2016).

50. Zhao, S. *et al.* Synthesis of micro/mesoporous silica material by duallate method as a heterogeneous catalyst support for alkylation. *RSC Adv.* **5**, 28124–28132 (2015).

51. Niu, D., Ma, Z., Li, Y. & Shi, J. Synthesis of core-shell structured dual-mesoporous silica spheres with tunable pore size and controllable shell thickness. *J. Am. Chem. Soc.* **132**, 15144–15147 (2010).

52. Sun, J. H., Shan, Z., Maschmeyer, T. & Coppens, M. O. Synthesis of bimodal nanostructured silicas with independently controlled small and large mesopore sizes. *Langmuir* **19**, 8395–8402 (2003).

53. Sun, J., Shan, Z., Maschmeyer, T., Moulijn, J. A. & Coppens, M. O. Synthesis of tailored bimodal mesoporous materials with independent control of the dual pore size distribution. *Chem. Commun.* **24**, 2670–2671 (2001).

54. Groenewolt, M., Antonietti, M. & Polarz, S. Mixed micellar phases of nonmiscible surfactants: Mesoporous silica with bimodal pore size distribution via the nanocasting process. *Langmuir* **20**, 7811–7819 (2004).

55. Dreiss, C. A. & Feng, Y. *Wormlike Micelles: Advances in Systems, Characterisation and Applications*. (Royal Society of Chemistry, 2017). doi:10.1016/b978-1-78242-325-6.01001-x.

56. Galgano, P. D. & El Seoud, O. A. Micellar properties of surface active ionic liquids: A comparison of 1-hexadecyl-3-methylimidazolium chloride with structurally related cationic surfactants. *J. Colloid Interface Sci.* **345**, 1–11 (2010).

57. Blin, J. L., Henzel, N. & Stébé, M. J. Mixed fluorinated-hydrogenated surfactant-based system: Preparation of ordered mesoporous materials. *J. Colloid Interface Sci.* **302**, 643–650 (2006).

58. Barthélémy, P., Tomao, V., Selb, J., Chaudier, Y. & Pucci, B. Fluorocarbon-hydrocarbon nonionic surfactants mixtures: A study of their miscibility. *Langmuir* **18**, 2557–2563 (2002).

59. Yang, Z. Z., He, L. N., Gao, J., Liu, A. H. & Yu, B. Carbon dioxide utilization with C-N bond formation: Carbon dioxide capture and subsequent conversion. *Energy Environ. Sci.* **5**, 6602–6639 (2012).

60. Asakawa, T., Hisamatsu, H. & Miyagishi, S. Micellar Pseudophase Separation Regions of 1H,1H,2H,2H-Perfluoroalkylpyridinium Chloride and Hydrocarbon Surfactants by Group Contribution Method. *Langmuir* **11**, 478–482 (1995).

61. Li, W., Zhang, M., Zhang, J. & Han, Y. Self-assembly of cetyl trimethylammonium bromide in ethanol-water mixtures. *Front. Chem. China* **1**, 438–442 (2006).

62. Aguiar, J., Carpena, P., Molina-Bolívar, J. A. & Carnero Ruiz, C. On the determination of the critical micelle concentration by the pyrene 1:3 ratio method. *J. Colloid Interface Sci.* **258**, 116–122 (2003).

63. Wang, T., Kaper, H., Antonietti, M. & Smarsly, B. Templating behavior of a long-chain ionic liquid in the hydrothermal synthesis of mesoporous silica. *Langmuir* **23**, 1489–1495 (2007).

64. Mukhim, T., Dey, J., Das, S. & Ismail, K. Aggregation and adsorption behavior of cetylpyridinium chloride in aqueous sodium salicylate and sodium benzoate solutions. *J. Colloid Interface Sci.* **350**, 511–515 (2010).

65. Tan, B., Vyas, S. M., Lehmler, H. J., Knutson, B. L. & Rankin, S. E. Unusual dependence of particle architecture on surfactant concentration in partially fluorinated decylpyridinium templated silica. *J. Phys. Chem. B* **109**, 23225–23232 (2005).

66. Tan, B., Dozier, A., Lehmler, H. J., Knutson, B. L. & Rankin, S. E. Elongated silica nanoparticles with a mesh phase mesopore structure by fluorosurfactant templating. *Langmuir* **20**, 6981–6984 (2004).

67. Gérardin, C., Reboul, J., Bonne, M. & Lebeau, B. Ecodesign of ordered mesoporous silica materials. *Chem. Soc. Rev.* **42**, 4217–4255 (2013).